Inorg. Chem. **2002**, *41*, 4114–4126

Synthesis, Characterization, and Solution Redox Properties of (trimpsi)M(CO)$_2$(NO) Complexes [M = V, Nb, Ta; trimpsi = ^{t}BuSi(CH$_2$PMe$_2$)$_3$]

Trevor W. Hayton, P. James Daff, Peter Legzdins,* Steven J. Rettig,† and Brian O. Patrick

Department of Chemistry, The University of British Columbia, Vancouver, British Columbia, Canada V6T 1Z1

Received January 14, 2002

Treatment of [Et$_4$N][M(CO)$_6$] (M = Nb, Ta) with I_2 in DME at –78 °C produces solutions of the bimetallic anions [M$_2$(μ-I)$_3$(CO)$_8$]$^-$. Addition of the tripodal phosphine ^{t}BuSi(CH$_2$PMe$_2$)$_3$ (trimpsi) followed by refluxing affords (trimpsi)M(CO)$_3$I [M = Nb (**1**), Ta (**2**)], which are isolable in good yields as air-stable, orange-red microcrystalline solids. Reduction of these complexes with 2 equiv of Na/Hg, followed by treatment with Diazald in THF, results in the formation of (trimpsi)M(CO)$_2$(NO) [M = Nb (**3**), Ta (**4**)] in high isolated yields. The congeneric vanadium complex, (trimpsi)V(CO)$_2$(NO) (**5**), can be prepared by reacting [Et$_4$N][V(CO)$_6$] with [NO][BF$_4$] in CH$_2$Cl$_2$ to form V(CO)$_5$(NO). These solutions are treated with 1 equiv of trimpsi to obtain (η^2-trimpsi)V(CO)$_3$(NO). Refluxing orange THF solutions of this material affords **5** in moderate yields. Reaction of (trimpsi)VCl$_3$(THF) (**6**) with 4 equiv of sodium naphthalenide in THF in the presence of excess CO provides [Et$_4$N][(trimpsi)V(CO)$_3$] (**7**), (trimpsi)V(CO)$_3$H, and [(trimpsi)V(μ-Cl)$_3$V(trimpsi)][(η^2-trimpsi)V(CO)$_4$]·3THF ([**8**][**9**]·3THF). All new complexes have been characterized by conventional spectroscopic methods, and the solid-state molecular structures of **2**·$^1/_2$THF, **3**–**5**, and [**8**][**9**]·3THF have been established by X-ray diffraction analyses. The solution redox properties of **3**–**5** have also been investigated by cyclic voltammetry. Cyclic voltammograms of **3** and **4** both exhibit an irreversible oxidation feature in CH$_2$Cl$_2$ ($E_{p,a}$ = –0.71 V at 0.5 V/s for **3**, while $E_{p,a}$ = –0.55 V at 0.5 V/s for **4**), while cyclic voltammograms of **5** in CH$_2$Cl$_2$ show a reversible oxidation feature ($E_{1/2}$ = –0.74 V) followed by an irreversible feature (0.61 V at 0.5 V/s). The reversible feature corresponds to the formation of the 17e cation [(trimpsi)V(CO)$_2$(NO)]$^+$ ([**5**]$^+$), and the irreversible feature likely involves the oxidation of [**5**]$^+$ to an unstable 16e dication. Treatment of **5** with [Cp$_2$Fe][BF$_4$] in CH$_2$Cl$_2$ generates [**5**][BF$_4$], which slowly decomposes once formed. Nevertheless, [**5**][BF$_4$] has been characterized by IR and ESR spectroscopies.

Introduction

When compared to nitrosyl complexes of metals from groups 6−10, the chemistry of group 5 nitrosyl complexes is relatively poorly developed.[1] The principal reasons for this state of affairs are (1) the group 5 metals are very oxophilic, (2) most nitrosylating agents are potent oxidizers and potential oxygen-atom sources, and (3) low-valent early-metal chemistry is itself relatively poorly developed. For instance, nitric oxide (NO), a common nitrosylating agent for the late metals,[1] typically reacts with early metal complexes to form oxo-containing compounds. Thus, reaction of Cp$_2$Zr(PMe$_3$)$_2$ with excess NO leads to the formation of [Cp$_2$Zr=O]$_x$ and N$_2$O,[2] and treatment of (silox)$_3$Nb(η^2-*N*,*C*-4-NC$_5$H$_4$Me) (silox = OSi^{t}Bu$_3$) with NO readily affords (silox)$_3$Nb=O, N$_2$, and 4-picoline.[3] Similarly, the reaction of Cp*$_2$VCl$_2$ with NO produces Cp*VCl$_2$(O), [Cp*VCl(μ-O)]$_4$, and N$_2$O.[4]

We, and other early-metal chemists, have recently begun to overcome these factors as evinced by our recent com-

* To whom correspondence should be addressed. E-mail: legzdins@chem.ubc.ca.

† Deceased October 27, 1998.

(1) (a) Richter-Addo, G. B.; Legzdins, P. *Metal Nitrosyls*; Oxford University Press: New York, 1992. (b) Hayton, T. W.; Legzdins, P.; Sharp, W. B. *Chem. Rev.* **2002**, *102*, 935−992.

(2) McNeill, K.; Bergman, R. G. *J. Am. Chem. Soc.* **1999**, *121*, 8260−8269.

(3) Veige, A. S.; Kleckley, T. S.; Chamberlin, R. M.; Neithamer, D. R.; Lee, C. E.; Wolczanski, P. T.; Lobkovsky, E. B.; Glassey, W. V. *J. Organomet. Chem.* **1999**, *591*, 194−203.

10.1021/ic020041r CCC: $22.00
Published on Web 06/26/2002

Scheme 1

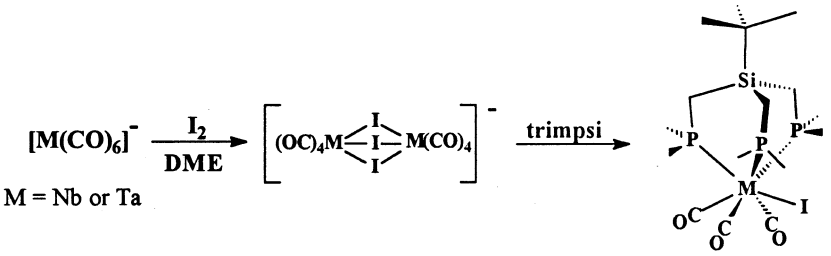

Nb **1**; Ta **2**

munication of the first nitrosyl complexes of niobium and tantalum, (trimpsi)M(CO)$_2$(NO) (trimpsi = ^{t}BuSi(CH$_2$PMe$_2$)$_3$; M = Nb, Ta).[5] Shortly thereafter, Ellis and coworkers synthesized the first dinitrosyls of these metals, namely [M(CNAr)$_4$(NO)$_2$]$^+$ (Ar = 2,6-Me$_2$C$_6$H$_3$).[6] They also prepared a second mononitrosyl of tantalum having the composition Ta(CNAr)$_5$(NO) (Ar = 2,6-Me$_2$C$_6$H$_3$).[7]

In this report we provide full details of the synthesis and characterization of (trimpsi)M(CO)$_2$(NO) (M = Nb, Ta; trimpsi = ^{t}BuSi(CH$_2$PMe$_2$)$_3$) and their precursors (trimpsi)M(CO)$_3$I. In addition, we describe the preparation of the remaining congener of the (trimpsi)M(CO)$_2$(NO) series, namely (trimpsi)V(CO)$_2$(NO), and outline the redox properties of all three dicarbonylnitrosyls as established by cyclic voltammetry.

Results and Discussion

(trimpsi)M(CO)$_2$(NO) (M = Nb, Ta). Our initial attempts to make niobium and tantalum nitrosyls focused on nitrosylating cyclopentadienyl-containing complexes with NO or nitrosyl chloride (ClNO). However, these efforts did not result in the preparation of the desired compounds. For instance, the reaction of Cp*MCl$_4$ (M = Nb, Ta) with excess NO in the presence of Zn, Al, or Na/Hg failed to generate any nitrosyl compounds. Treatment of lower oxidation-state precursors such as Cp*Ta(CO)$_2$Cl$_2$(THF) with NO also failed to produce nitrosyl-containing complexes. We surmise that the products from these reactions consist of high-valent, oxo-containing species.[2−4]

We reasoned that NO was too strong an oxidant to be used with early metal complexes. Consequently, we devised a synthetic route using Diazald (*N*-methyl-*N*-nitroso-*p*-toluenesulfonamide), a nonoxidative nitrosylating agent with which we are familiar.[8] This route involves reacting [Et$_4$N][M(CO)$_6$] (M = Nb, Ta)[9,10] with I$_2$ in 1,2-dimethoxyethane (DME) at −78 °C to produce the bimetallic anions [M$_2$(μ-I)$_3$(CO)$_8$]$^-$ (Scheme 1).[11] Treatment of these solutions with trimpsi at −78 °C followed by refluxing for 2 h generates (trimpsi)M(CO)$_3$I [M = Nb (**1**), Ta (**2**)]. Crystallization from DME affords **1** and **2** in good yields (**1**, 82%; **2**, 84%) as air-stable, orange-red microcrystalline solids.

Table 1. Selected Bond Lengths (Å) and Angles (deg) for (trimpsi)Ta(CO)$_3$I (**2**)

Bond Lengths			
Ta(1)−I(1)	2.9540(3)	Ta(1)−C(15)	2.010(4)
Ta(1)−P(1)	2.6350(9)	Ta(1)−C(16)	2.066(4)
Ta(1)−P(2)	2.6803(11)	C(14)−O(1)	1.155(5)
Ta(1)−P(3)	2.5784(9)	C(15)−O(2)	1.174(6)
Ta(1)−C(14)	2.050(4)	C(16)−O(3)	1.153(5)

Bond Angles			
I(1)−Ta(1)−P(1)	88.11(2)	P(2)−Ta(1)−C(14)	159.66(12)
I(1)−Ta(1)−P(2)	87.67(2)	P(2)−Ta(1)−C(15)	128.15(11)
I(1)−Ta(1)−P(3)	164.72(2)	P(2)−Ta(1)−C(16)	81.38(12)
I(1)−Ta(1)−C(14)	77.16(11)	P(3)−Ta(1)−C(14)	110.63(12)
I(1)−Ta(1)−C(15)	123.99(10)	P(3)−Ta(1)−C(15)	71.29(10)
I(1)−Ta(1)−C(16)	76.44(11)	P(3)−Ta(1)−C(16)	112.04(10)
P(1)−Ta(1)−P(2)	86.84(3)	C(14)−Ta(1)−C(15)	72.11(16)
P(1)−Ta(1)−P(3)	80.75(3)	C(14)−Ta(1)−C(16)	107.60(15)
P(1)−Ta(1)−C(14)	79.28(11)	C(15)−Ta(1)−C(16)	70.11(17)
P(1)−Ta(1)−C(15)	128.77(12)	Ta(1)−C(14)−O(1)	177.8(4)
P(1)−Ta(1)−C(16)	160.86(12)	Ta(1)−C(15)−O(2)	175.9(3)
P(2)−Ta(1)−P(3)	81.34(3)	Ta(1)−C(16)−O(3)	178.3(4)

The IR spectra of **1** and **2** (Nujol mulls) exhibit three strong bands in the carbonyl-stretching region, namely 1938, 1846, and 1800 cm^{-1} for **1** and 1928, 1838, and 1793 cm^{-1} for **2**. These spectra are qualitatively similar to those exhibited by the related TaX(PMe$_3$)$_3$(CO)$_3$ complexes (X = Cl, Br, I).[12,13] The ^{31}P{^{1}H} NMR spectra of both **1** and **2** in CD$_2$Cl$_2$ each consist of a broad singlet at 25 °C, indicating that the complexes are stereochemically nonrigid in solution. Consistently, their ^{1}H and ^{13}C NMR spectra also exhibit signals reflecting intramolecular exchange of the ligands in the metals' coordination spheres. Crystals of **2**·$^1/_2$THF were grown from THF/hexanes (3:1) and contain a half molecule of THF in the lattice as evinced by a single-crystal X-ray crystallographic analysis. An ORTEP diagram of (trimpsi)Ta(CO)$_3$I is shown in Figure 1, and selected bond lengths and angles are collected in Table 1. Qualitatively, the complex has a 4:3 "piano stool" structure.[14] Alternatively,

(4) Bottomley, F.; Darkwa, J.; Sutin, L.; White, P. S. *Organometallics* **1986**, *5*, 2165−2171.
(5) Daff, P. J.; Legzdins, P.; Rettig, S. J. *J. Am. Chem. Soc.* **1998**, *120*, 2688−2689.
(6) Barybin, M. V.; Young, V. G., Jr.; Ellis, J. E. *Organometallics* **1999**, *18*, 2744−2746.
(7) Barybin, M. V.; Young, V. G., Jr.; Ellis, J. E. *J. Am. Chem. Soc.* **1999**, *121*, 9237−9238.
(8) Legzdins, P.; Veltheer, J. E. *Acc. Chem. Res.* **1993**, *26*, 41−48.
(9) Dewey, C. G.; Ellis, J. E.; Fjare, K. L.; Pfahl, K. M.; Warnock, G. F. P. *Organometallics* **1983**, *2*, 388−391.
(10) Ellis, J. E.; Warnock, G. F. P.; Barybin, M. V.; Pomije, M. K. *Chem.*−*Eur. J.* **1995**, *1*, 521−527.
(11) Calderazzo, F.; Castellani, M.; Pampaloni, G.; Zanazzi, P. F. *J. Chem. Soc., Dalton Trans.* **1985**, 1989−1995.
(12) Luetkens, M. L., Jr.; Santure, D. J.; Huffman, J. C.; Sattelberger, A. P. *J. Chem. Soc., Chem. Commun.* **1985**, 552−553.
(13) Luetkens, M. L., Jr.; Hopkins, M. D.; Schultz, A. J.; Williams, J. M.; Fair, C. K.; Ross, F. K.; Huffman, J. C.; Sattelberger, A. P. *Inorg. Chem.* **1987**, *26*, 2430−2436.
(14) Dreyer, E. B.; Lam, C. T.; Lippard, S. J. *Inorg. Chem.* **1979**, *18*, 1904−1908.

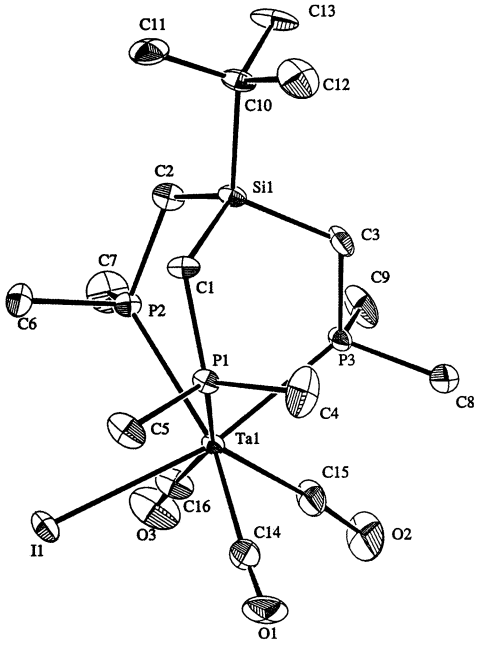

Figure 1. ORTEP plot of the solid-state molecular structure of (trimpsi)-$Ta(CO)_3I$ (**2**) with 50% probability ellipsoids.

the coordination geometry at the tantalum center can be described as a capped trigonal prism with I(1) forming the cap and P(1), P(2), C(16), and C(14) forming the rectangular face. As expected, P(3), which lies roughly trans to the iodo ligand, exhibits a shorter Ta−P bond length [Ta(1)−P(3) = 2.578(1) Å] relative to P(1) [Ta(1)−P(1) = 2.635(1) Å] and P(2) [Ta(1)−P(2) = 2.680(1) Å]. The carbonyl ligands which are approximately trans to each other exhibit longer Ta−C bonds [Ta(1)−C(14) = 2.050(4) Å, Ta(1)−C(16) = 2.066-(4) Å] than does the carbonyl ligand trans to iodide [Ta-(1)−C(15) = 2.010(4) Å]. The three C−O distances are all equivalent by the 3σ criterion and are comparable to those exhibited by $TaCl(PMe_3)_3(CO)_3$ and $[Ta(CO)_3(PMe_3)_4]^+$.[13,15]

Solutions of **1** and **2** in DME can be reduced with 2 equiv of Na/Hg at ambient temperature to form [Na][(trimpsi)-$M(CO)_3$] (Scheme 2). These anions react with 1 equiv of Diazald to generate deep-red solutions of (trimpsi)$M(CO)_2$-(NO) [M = Nb (**3**), Ta (**4**)]. Recrystallization from THF/hexanes (2:1) or MeCN provides crystalline samples of **3** and **4** in 88% and 90% yields, respectively.

The IR spectra of **3** and **4** (Nujol mulls) reveal exceptionally low ν(NO) values of 1518 and 1515 cm^{-1}, respectively, lower in energy than that reported for the only other known mononitrosyl of Nb or Ta, namely 1542 cm^{-1} (THF solution) for $Ta(NO)(CNAr)_5$ (Ar = 2,6-$Me_2C_6H_3$).[7] The ν(CO) values for **3** (1908 and 1821 cm^{-1}) and **4** (1895 and 1802 cm^{-1}) are comparable to those exhibited by other electron-rich group 5 carbonyls. For instance, the ν(CO) value of $[Ta(CO)_6]^-$ is 1835 cm^{-1} (Nujol mull).[9] The room-temperature $^{31}P\{^1H\}$ NMR spectrum of **3** in CD_2Cl_2 appears as a single broad complex feature centered at −20 ppm, suggesting overlapping ^{31}P resonances. The $^{31}P\{^1H\}$ NMR spectrum

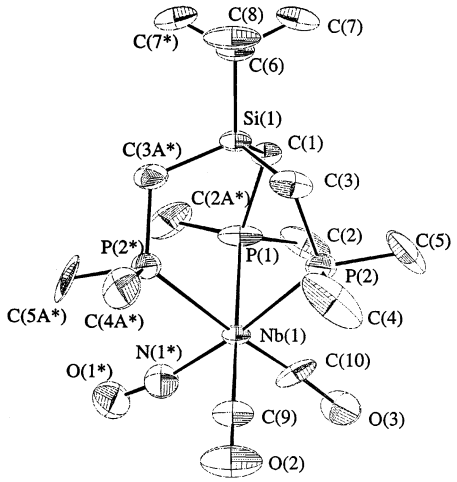

Figure 2. ORTEP plot of the solid-state molecular structure of (trimpsi)-$Nb(CO)_2(NO)$ (**3**) with 50% probability ellipsoids. Asterisks indicate symmetry-related atoms, and the CO and NO ligands are mutually disordered.

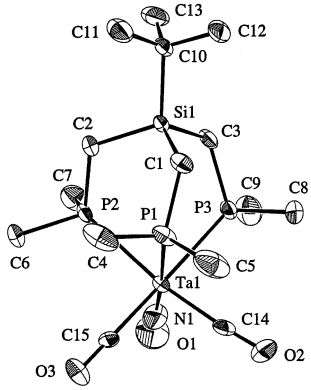

Figure 3. ORTEP plot of the solid-state molecular structure of (trimpsi)-$Ta(CO)_2(NO)$ (**4**) with 50% probability ellipsoids.

of **4** is much simpler, consisting of two singlets at −24.0 ppm (2P) and −33.2 ppm (1P). The room-temperature $^{93}Nb-\{^1H\}$ NMR spectrum of **3** in CD_2Cl_2 consists of a broad singlet (fwhh = 4800 Hz) at −1493 ppm, in the same region as the chemical shifts reported for other low-valent Nb complexes.[16,17]

X-ray crystallographic analyses of single crystals of **3** and **4** have been performed, and the resulting ORTEP diagrams are shown in Figures 2 and 3, respectively. Selected bond lengths and angles of the molecules shown are presented in Tables 2 and 3, respectively. The solid-state molecular structures reveal the expected octahedral coordination geometries with linear nitrosyl ligands [Nb(1)−N(1)−O(1) = 168.7(16)°; Ta(1)−N(1)−O(1) = 170(2)°]. The structure of **3** contains a crystallographically imposed mirror plane. Contrary to our initial expectations that the nitrosyl ligand would be situated in the mirror plane,[5] the structure of **3** refines best with one CO ligand lying in the mirror plane and the remaining two EO (E = C or N) ligand sites being

(15) Luetkens, M. L., Jr.; Huffman, J. C.; Sattelberger, A. P. *J. Am. Chem. Soc.* **1985**, *107*, 3361−3363.

(16) Rehder, D.; Bechthold, H.-C.; Keçeci, A.; Schmidt, H.; Siewing, M. *Z. Naturforsch., B: Chem. Sci.* **1982**, *37*, 631−645.

(17) Rehder, D.; Rodewald, D. In *Advanced Application of NMR to Organometallic Chemistry*; Gielen, M., Willem, R., Wrackmeyer, B., Eds.; John Wiley & Sons: New York, 1996; Vol. 1, pp 291−311.

Scheme 2

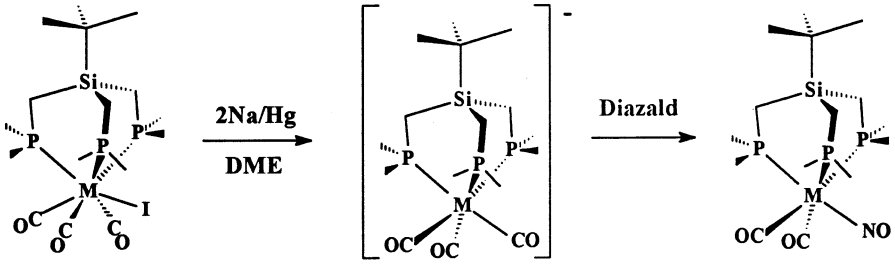

Table 2. Selected Bond Lengths (Å) for (trimpsi)Nb(CO)$_2$(NO) (**3**), (trimpsi)Ta(CO)$_2$(NO) (**4**), and (trimpsi)V(CO)$_2$(NO) (**5**)

3		**4**		**5**	
Nb(1)−P(1)	2.578(1)	Ta(1)−P(1)	2.583(2)	V(1)−P(1)	2.495(2)
Nb(1)−P(2)	2.635(1)	Ta(1)−P(2)	2.620(2)	V(1)−P(2)	2.482(2)
Nb(1)−C(9)	2.084(6)	Ta(1)−P(3)	2.612(2)	V(1)−P(3)	2.434(2)
Nb(1)−C(10)	1.79(3)	Ta(1)−C(14)	1.94(1)	V(1)−C(14)	1.926(7)
Nb(1)−N(1)	2.050(12)	Ta(1)−C(15)	1.93(1)	V(1)−C(15)	1.841(9)
C(9)−O(2)	1.148(7)	Ta(1)−N(1)	2.16(2)	V(1)−N(1)	1.823(9)
C(10)−O(1)	1.54(2)	C(14)−O(2)	1.24(1)	C(14)−O(2)	1.166(9)
C(10)−O(3)	1.30(3)	C(15)−O(3)	1.22(1)	C(15)−O(3)	1.17(1)
N(1)−O(1)	1.19(2)	N(1)−O(1)	0.99(2)	N(1)−O(1)	1.24(1)

equally occupied by NO and CO ligands. Nevertheless, it is likely that the nitrosyl ligand actually occupies all three nonphosphine ligand sites. Furthermore, the trimpsi ligand in **3** exhibits disorder brought about by either a left or right twist of the trimpsi ligand about the Si(1)−Nb(1) axis such that two orientations of the CH_2PMe_2 arms are possible.[18] This disorder in **3** results in a degree of uncertainty being associated with the determined intramolecular metrical parameters. Nevertheless, the dimensions of **3** generally compare well to those of other low-valent Nb phosphine complexes. The Nb(1)−N(1) bond length of 2.05(1) Å in **3** is shorter than that of a typical Nb−N single bond (2.3−2.5 Å) and is consistent with the existence of Nb−N multiple-bond character resulting from Nb → NO back-bonding. However, it is rather long when compared to typical M−N distances in metal nitrosyls which are usually 1.65−1.80 Å.[19] This feature is likely an artifact of the aforementioned disorder. The N(1)−O(1) bond length in **3** is found to be 1.19(2) Å, also shorter than expected given the electron-rich nature of the Nb center. Similar disorder is evident in the solid-state molecular structure of **4** which does not possess a crystallographic plane of symmetry. Consequently, its Ta−N and N−O bond parameters are again much different than expected (Table 2).

To put these metrical parameters of **3** and **4** in perspective, it should be noted that Ta(CNAr)$_5$(NO) exhibits a Ta−N distance of 1.897(12) Å and an N−O distance of 1.214(14) Å, much shorter and longer, respectively, than those found for either **3** or **4**.[7] Indeed, these dimensions are more in line with expectation considering the high electron density on the Ta center. Consistently, the M−N distances [Nb−N = 1.887(2) and 1.889(2) Å; Ta−N = 1.902(5) and 1.914(5) Å] and the N−O distances (NbN−O = 1.183(3) and 1.186-(3) Å; TaN−O = 1.182(6) and 1.193(6) Å] in the dinitrosyls [M(NO)$_2$(CNAr)$_4$]$^-$ are dramatically different from those in **3** and **4**.[6]

(trimpsi)V(CO)$_2$(NO). In light of the significance of **3** and **4** to metal nitrosyl chemistry, we felt justified in trying to synthesize the vanadium congener. In contrast to niobium and tantalum, for which only five nitrosyl complexes are known, there are many known vanadium nitrosyl complexes.[1] The first such complex was K$_3$[V(CN)$_5$(NO)], prepared by Wilkinson and co-workers in 1959 from the reaction of [NH$_4$]-[VO$_3$] with hydroxylamine and KCN[20] and subsequently characterized structurally by Jagner and co-workers.[21,22] Also known is its seven-coordinate KCN adduct K$_4$[V(CN)$_6$-(NO)].[23,24] A number of other vanadium nitrosyl complexes have been formed similarly by reacting a vanadium oxo species with hydroxylamine,[25−27] and several of these have been structurally characterized.[28−31] The reaction between Cp′$_2$VX (X = Cl, Br, I) and NO also generates a number of nitrosyl-containing products, including the crystallographically characterized cluster (CpVI)$_2$(CpV(NO))$_2$(μ-O)$_4$.[32−34] Many of these complexes are formed in aqueous solutions and are oxygen and water stable. It thus appears that vanadium nitrosyls are more accessible than are their Nb and Ta counterparts.

(18) Gardner, T. G.; Girolami, G. S. *Organometallics* **1987**, *6*, 2551−2556.
(19) Feltham, R. D.; Enemark, J. H. *Top. Stereochem.* **1981**, *12*, 155−215.
(20) Griffith, W. P.; Lewis, J.; Wilkinson, G. *J. Chem. Soc.* **1959**, 1632−1633.
(21) Jagner, S.; Vannerberg, N. *Acta Chem. Scand.* **1968**, *22*, 3330−3331.
(22) Jagner, S.; Vannerberg, N. *Acta Chem. Scand.* **1970**, *24*, 1988−2002.
(23) Müller, A.; Werle, P.; Diemann, E.; Aymonino, P. J. *Chem. Ber.* **1972**, *105*, 2419−2420.
(24) Drew, M. G. B.; Pygall, C. F. *Acta Crystallogr., Sect. B* **1977**, *B33*, 2838−2842.
(25) Quilitzsch, U.; Wieghardt, K. *Z. Naturforsch., B: Chem. Sci.* **1979**, *34*, 640−641.
(26) Wieghardt, K.; Quilitzsch, U. *Z. Anorg. Allg. Chem.* **1979**, *457*, 75−83.
(27) Mallik, M.; Ghosh, P. N.; Bhattacharyya, R. *J. Chem. Soc., Dalton. Trans.* **1993**, 1731−1736.
(28) Wieghardt, K.; Quilitzsch, U.; Nuber, B.; Weiss, J. *Angew. Chem., Int. Ed. Engl.* **1978**, *17*, 351−352.
(29) Wieghardt, K.; Kleine-Boymann, M.; Swiridoff, W.; Nuber, B.; Weiss, J. *J. Chem. Soc., Dalton. Trans.* **1985**, 2493−2497.
(30) Hauser, C.; Weyhermuller, T.; Wieghardt, K. *Collect. Czech. Chem. Commun.* **2001**, *66*, 125−138.
(31) Kitagawa, S.; Munakata, M.; Ueda, M. *Inorg. Chim. Acta* **1989**, *164*, 49−53.
(32) Bottomley, F.; Darkwa, J.; White, P. S. *J. Chem. Soc., Chem. Commun.* **1982**, 1039−1040.
(33) Bottomley, F.; Darkwa, J.; White, P. S. *Organometallics* **1985**, *4*, 961−965.
(34) Bottomley, F.; Darkwa, J.; White, P. S. *J. Chem. Soc., Dalton. Trans.* **1985**, 1435−1442.

Table 3. Selected Bond Angles (deg) for (trimpsi)$Nb(CO)_2(NO)$ (**3**), (trimpsi)$Ta(CO)_2(NO)$ (**4**), and (trimpsi)$V(CO)_2(NO)$ (**5**)

3		**4**		**5**	
P(1)−Nb(1)−N(1)	94.8(4)	P(1)−Ta(1)−P(2)	83.17(5)	P(1)−V(1)−P(2)	86.72(6)
P(2)−Nb(1)−N(1)	173.0(5)	P(1)−Ta(1)−P(3)	86.85(5)	P(1)−V(1)−P(3)	85.99(8)
P(1)−Nb(1)−C(9)	179.0(2)	P(1)−Ta(1)−C(14)	95.1(3)	P(1)−V(1)−C(14)	93.0(3)
P(2)−Nb(1)−C(10)	96(1)	P(1)−Ta(1)−C(15)	91.5(3)	P(1)−V(1)−C(15)	175.1(3)
C(10)−Nb(1)−N(1)	90.6(6)	P(1)−Ta(1)−N(1)	175.4(6)	P(1)−V(1)−N(1)	90.8(3)
C(10)−Nb(1)−C(9)	92.7(7)	P(2)−Ta(1)−P(3)	85.95(5)	P(2)−V(1)−P(3)	87.25(8)
N(1)−Nb(1)−C(9)	85.8(4)	P(2)−Ta(1)−C(14)	170.8(4)	P(2)−V(1)−C(14)	93.6(3)
P(1)−Nb(1)−C(10)	88.0(7)	P(2)−Ta(1)−C(15)	93.5(4)	P(2)−V(1)−C(15)	88.5(3)
P(2)−Nb(1)−C(9)	94.9(1)	P(2)−Ta(1)−N(1)	92.3(6)	P(2)−V(1)−N(1)	176.9(3)
P(2)−Nb(1)−P(1)	84.38(4)	P(3)−Ta(1)−C(14)	84.9(4)	P(3)−V(1)−C(14)	178.6(4)
P(2)−Nb(1)−P(2)*	84.44(6)	P(3)−Ta(1)−C(15)	178.3(4)	P(3)−V(1)−C(15)	92.9(3)
Nb(1)−N(1)−O(1)	169(2)	P(3)−Ta(1)−N(1)	92.4(5)	P(3)−V(1)−N(1)	90.7(3)
Nb(1)−C(10)−O(3)	171(2)	N(1)−Ta(1)−C(14)	89.4(7)	N(1)−V(1)−C(14)	88.4(4)
Nb(1)−C(9)−O(2)	173.5(6)	N(1)−Ta(1)−C(15)	89.1(6)	N(1)−V(1)−C(15)	94.0(3)
		C(14)−Ta(1)−C(15)	95.5(5)	C(14)−V(1)−C(15)	88.2(4)
		Ta(1)−C(14)−O(2)	168(1)	V(1)−C(14)−O(2)	173.0(7)
		Ta(1)−C(15)−O(3)	171.4(9)	V(1)−C(15)−O(3)	176.2(8)
		Ta(1)−N(1)−O(1)	170(2)	V(1)−N(1)−O(1)	179.1(8)

Scheme 3

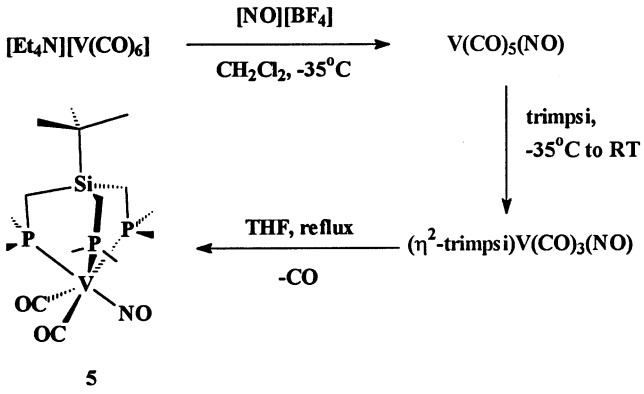

5

Our first attempts at forming (trimpsi)$V(CO)_2(NO)$ consisted of simply repeating the procedure used to make **3** and **4** (Scheme 1) by using $[Et_4N][V(CO)_6]$ as the starting material. However, all attempts to form (trimpsi)$V(CO)_3I$ by this method failed, and instead the known (trimpsi)$V(CO)_3H$ was isolated in low yield.[18] Presumably, the seven-coordinate (trimpsi)$V(CO)_3I$ is initially formed but then loses $I^{\bullet}$ and abstracts a hydrogen atom from DME.

We then turned our attention to $V(CO)_5(NO)$ as a possible precursor. This complex was first formed by treating $V(CO)_6$ with NO in cyclohexane.[35] A more convenient method involves reacting $[V(CO)_6]^-$ with the nitrosonium salt $[NO][BF_4]$.[36] $V(CO)_5(NO)$ is thermally unstable both in solution and in the solid state, and it evolves CO above 0 °C. In the presence of Lewis bases such as phosphines, CO-substitution occurs and tractable 18e, octahedral complexes are formed.[36−38]

Treatment of a yellow CH_2Cl_2 solution of $[Et_4N][V(CO)_6]$ with a finely ground suspension of $[NO][BF_4]$ at −35 °C slowly generates a deep maroon solution of $V(CO)_5(NO)$ (Scheme 3). The reaction appears to be complete after about 8 h. If the reaction temperature rises above −20 °C at any point, the color of the solution quickly turns red-brown and lower yields of the final nitrosyl product are obtained. Also, if the $[NO][BF_4]$ reagent is not freshly sublimed and finely ground with mortar and pestle, the reaction rate is much slower and the isolated yields are much lower.

Addition of 1 equiv of trimpsi to solutions of $V(CO)_5(NO)$ in CH_2Cl_2 at −35 °C, followed by warming to room temperature, results in a color change from purple to orange with concomitant gas evolution. IR spectra of this orange material in THF suggest that it is best formulated as (η^2-trimpsi)$V(CO)_3(NO)$ since ν(CO) bands are evident at 1990, 1904, and 1813 cm^{-1} and ν(NO) occurs at 1600 cm^{-1}. This material is an oil, and no further attempts have been made to characterize it. Refluxing the oil in THF for 1 h results in the disappearance of the original ν(CO) and ν(NO) bands and the appearance of new ν(CO) bands at 1919 and 1833 cm^{-1} and a new ν(NO) absorption at 1560 cm^{-1}. These new IR bands are due to (trimpsi)$V(CO)_2(NO)$ (**5**), which can be recrystallized from MeCN or THF/hexanes in moderate yield.

The room-temperature $^{31}P\{^1H\}$ NMR spectrum of **5** in CD_2Cl_2 consists of two octets at 5 ppm (2P) and −10 ppm (1P), respectively (Figure 4). The $^{51}V-^{31}P$ coupling constants are 220 and 130 Hz for the phosphorus nuclei trans to the CO and NO ligands, respectively. These coupling constants are in accord with previously reported J_{VP} values.[18] The $^{51}V\{^1H\}$ NMR spectrum of **5** reveals a complex 14-line signal centered at −1315 ppm (Figure 5a), a chemical shift similar to that observed for (triphos)$V(CO)_2(NO)$ (triphos = $MeC(CH_2PPh_2)_3$) (−1242 ppm)[39] and $V(CO)_3L_2(NO)$-type (−1270 to −1480 ppm) complexes (L = neutral 2e donor).[40] The $^{51}V-^{14}N$ coupling constant is 115 Hz. Such V−N coupling has been observed for vanadium nitrosyls previously, but no coupling constants have been reported.[39,40] The $^{51}V\{^1H\}$ NMR spectrum of the ^{15}N isotopomer **5**-^{15}N consists of a seven-line signal, thereby confirming the existence of V−N coupling (Figure 5b). Regrettably, many attempts to detect a resonance for the ^{15}N nucleus of **5**-^{15}N by $^{15}N\{^1H\}$ NMR spectroscopy were unsuccessful.

Single crystals of **5** were grown from THF/hexanes (3:1) at −30 °C and were analyzed by X-ray crystallography. An

(35) Hieber, W.; Peterhans, J.; Winter, E. *Chem. Ber.* **1961**, *94*, 2572−2578.
(36) Fjare, K. L.; Ellis, J. E. *J. Am. Chem. Soc.* **1983**, *105*, 2303−2307.
(37) Shi, Q.; Richmond, T. G.; Trogler, W. C.; Basolo, F. *Inorg. Chem.* **1984**, *23*, 957−960.
(38) Töfke, S.; Behrens, U. *Acta Crystallogr., Sect. C* **1986**, *C42*, 161−163.
(39) Schiemann, J.; Weiss, E.; Näumann, F.; Rehder, D. *J. Organomet. Chem.* **1982**, *232*, 219−227.
(40) Rehder, D. *Magn. Reson. Rev.* **1984**, *9*, 125−237.

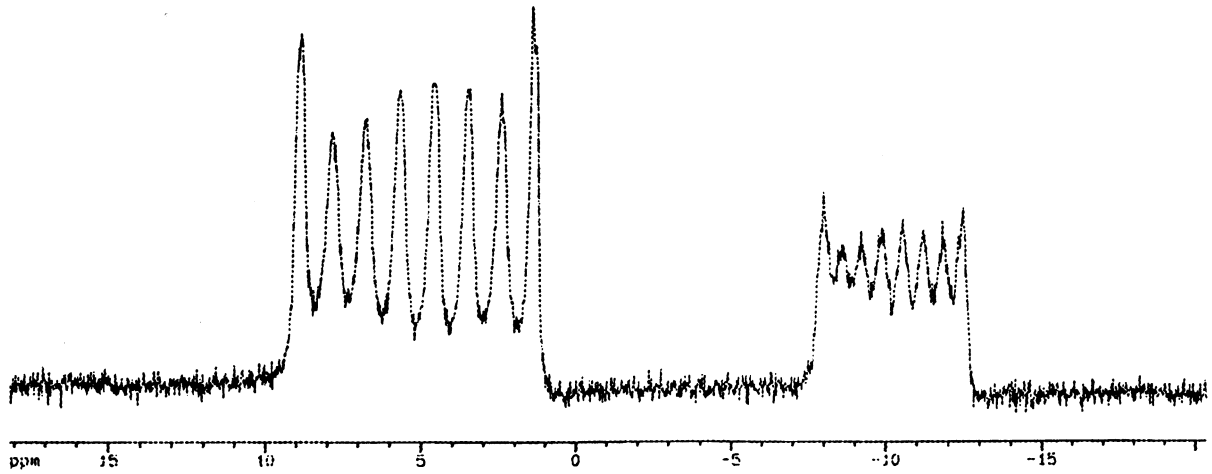

Figure 4. $^{31}P\{^1H\}$ NMR spectrum of **5** in CD_2Cl_2 at room temperature.

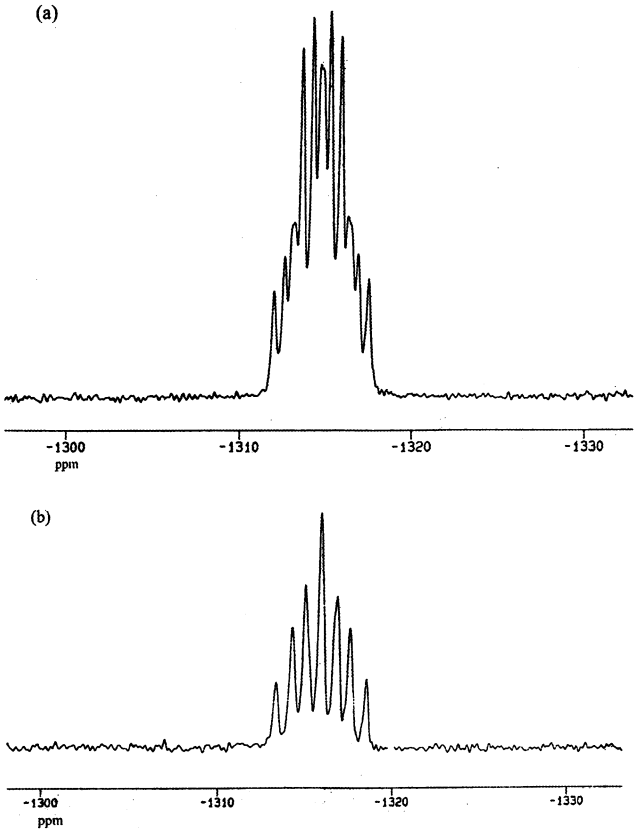

Figure 5. (a) $^{51}V\{^1H\}$ NMR spectrum of **5** in CD_2Cl_2. (b) $^{51}V\{^1H\}$ NMR spectrum of **5**-^{15}N in CD_2Cl_2.

ORTEP diagram of **5** is shown in Figure 6, and selected bond lengths and angles are collected in Tables 2 and 3, respectively. Complex **5** exhibits the expected octahedral coordination geometry, and the V−NO linkage is linear [V(1)−N(1)−O(1) = 179.1(8)°] with a V(1)−N(1) distance of 1.823(9) Å and a N(1)−O(1) distance of 1.24(1) Å. These bond lengths are similar to those exhibited by $V(CO)_4(PMe_3)$-(NO) and $V(CO)_3(PMe_3)_2(NO)$, which have V−N and N−O distances of 1.747(3) and 1.208(3) Å and 1.809(10) and 1.204(11) Å, respectively.[38,41] Again, the nitrosyl N−O distance extant in **5** is much different from the comparable parameters in **3** and **4**.

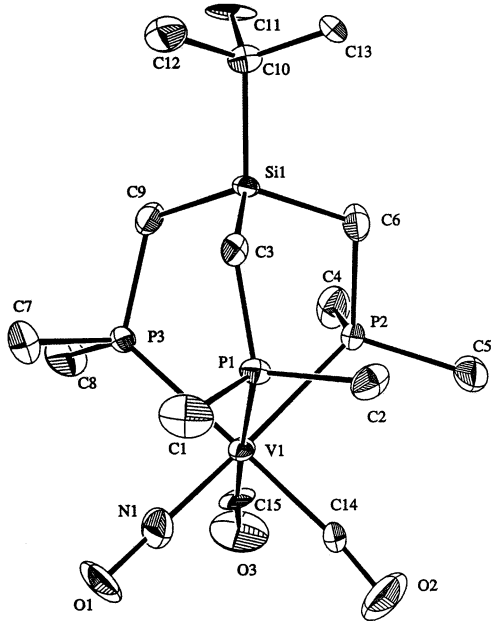

Figure 6. ORTEP plot of the solid-state molecular structure of (trimpsi)$V(CO)_2(NO)$ (**5**) with 50% probability ellipsoids.

[Et$_4$N][(trimpsi)V(CO)$_3$]. The moderate yield of **5** was of some concern; consequently, a higher-yielding preparative route was sought. Although the following route was ultimately unsuccessful in improving the yield of **5,** several new complexes were formed, and their syntheses and characterization are outlined in the following sections. In a procedure reminiscent of the synthesis of (trimpsi)$V(CO)_3H$,[18] (trimpsi)-$VCl_3(THF)$ (**6**) was reacted with 4 equiv of sodium naphthalenide in THF in the presence of excess CO (eq 1). After 24 h this solution was treated with $[Et_4N][Cl]$ and was stirred for another 24 h. Crystallization of the final residue from THF afforded $[Et_4N][(trimpsi)V(CO)_3]$ (**7**) as a yellow powder in 5% yield. Attempts to isolate further crops of **7** only resulted in the isolation of slightly impure (trimpsi)V-$(CO)_3H$, as indicated by its color.[18] Pure (trimpsi)$V(CO)_3H$ is normally yellow, whereas the isolated material had a definite greenish hue.

(41) Schiemann, J.; Weiss, E. *J. Organomet. Chem.* **1982**, *232*, 229−232.

$$\underset{\mathbf{6}}{(\text{trimpsi})VCl_3(THF)} \xrightarrow[\text{(ii) } [Et_4N][Cl]]{\text{(i) 4 Na/C}_{10}H_8\text{, xs CO, THF, } -78\ ^\circ C} \underset{\mathbf{7}}{[Et_4N][(\text{trimpsi})V(CO)_3]} + (\text{trimpsi})V(CO)_3H + \text{other products} \quad (1)$$

An IR spectrum of **7** (Nujol mull) contains three ν(CO) bands at 1780, 1680, and 1655 cm^{-1}. These absorptions are lower in energy than the carbonyl-stretching frequencies of (trimpsi)V(CO)$_3$H (1880 and 1785 cm^{-1}) and are comparable to the spectrum exhibited by [Cp*Ti(CO)$_2$(dmpe)]$^-$ [ν(CO) at 1680 and 1600 cm^{-1}].[42] The room-temperature ^{31}P{^{1}H} NMR spectrum of **7** in CD$_3$CN consists of an octet at 14.2 ppm with a ^{31}P$-^{51}$V coupling constant of 200 Hz.

Clearly, the very low yield of **7** prevents it from being a viable precursor for the synthesis of **5**. Nonetheless, equimolar amounts of **7** and [NO][BF$_4$] in CD$_3$CN react to give orange-red solutions containing **5** along with some decomposition products, as judged by ^{31}P{^{1}H} NMR spectroscopy (eq 2). A similar procedure has been used previously to synthesize (Me$_3$P)$_2$V(CO)$_3$(NO).[39]

$$\underset{\mathbf{7}}{[Et_4N][(\text{trimpsi})V(CO)_3]} + [NO][BF_4] \rightarrow \underset{\mathbf{5}}{(\text{trimpsi})V(CO)_2(NO)} + \text{decomposition} \quad (2)$$

[(trimpsi)V(μ-Cl)$_3$V(trimpsi)][(η^2-trimpsi)V(CO)$_4$]·3THF. As noted above, the (trimpsi)V(CO)$_3$H isolated during the synthesis of **7** via eq 1 is slightly impure. Purification of the yellow hydrido complex by recrystallization from THF was accompanied by the formation of a few green crystals. These crystals have been subjected to an X-ray crystallographic analysis which reveals them to be [(trimpsi)V(μ-Cl)$_3$V(trimpsi)][(η^2-trimpsi)V(CO)$_4$]·3THF ([**8**][**9**]·3THF). ORTEP diagrams of [**8**]$^+$ and [**9**]$^-$ are shown in Figures 7 and 8, respectively, and their selected bond lengths and angles are tabulated in Tables 4 and 5, respectively. The cation, [(trimpsi)V(μ-Cl)$_3$V(trimpsi)]$^+$ ([**8**]$^+$), consists of two face-sharing octahedra bridged by three chlorides and capped by two trimpsi ligands. It is structurally analogous to [(THF)$_3$V(μ-Cl)$_3$V(THF)$_3$]$^+$, an important synthon in low-valent vanadium chemistry[43] which has been structurally characterized numerous times.[44−50] In [(THF)$_3$V(μ-Cl)$_3$-V(THF)$_3$]$^+$ the average V−Cl bond length is 2.48 Å while the average V−Cl−V and Cl−V−Cl angles are 73.8 and 87.7°, respectively.[50] Almost identical parameters are evident in [**8**]$^+$, which exhibits an average V−Cl bond length of 2.46 Å and average V−Cl−V and Cl−V−Cl angles of 74.2 and 87.4°, respectively. Comparison of [**8**]$^+$ with [(PMe$_3$)$_3$V(μ-Cl)$_3$V(PMe$_3$)$_3$]$^+$, though, shows a slight difference in the V−P distances. The average V−P distance in [**8**]$^+$ is 2.50 Å while the average V−P distance in [(PMe$_3$)$_3$V(μ-Cl)$_3$-V(PMe$_3$)$_3$]$^+$ is 2.55 Å.[44]

The anion, [(η^2-trimpsi)V(CO)$_4$]$^-$ ([**9**]$^-$), in which one of the arms of trimpsi is pendant, is an 18e octahedral species, isoelectronic with [V(CO)$_6$]$^-$. To our knowledge, it represents the first structurally characterized phosphine-substituted derivative of [V(CO)$_6$]$^-$. Anion [**9**]$^-$ exhibits an average V−P bond length of 2.40 Å, shorter than that found in [**8**]$^+$, as

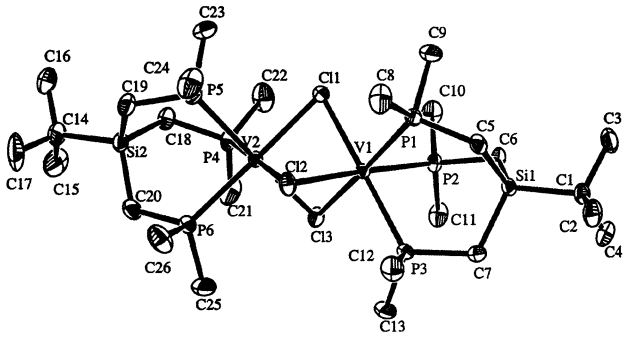

Figure 7. ORTEP plot of the solid-state molecular structure of [(trimpsi)-V(μ-Cl)$_3$V(trimpsi)] ([**8**]$^+$) with 50% probability ellipsoids.

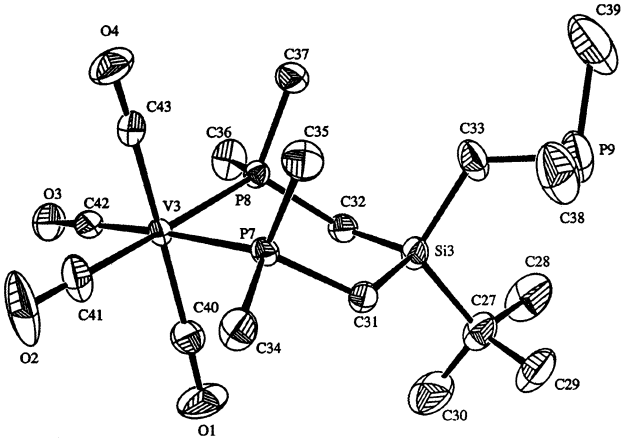

Figure 8. ORTEP plot of the solid-state molecular structure of [(η^2-trimpsi)V(CO)$_4$]$^-$ ([**9**]$^-$) with 50% probability ellipsoids.

Table 4. Selected Bond Lengths (Å) for [(trimpsi)V(μ-Cl)$_3$V(trimpsi)][(η^2-trimpsi)V(CO)$_4$] ([**8**][**9**])

[**8**]$^+$		[**9**]$^-$	
V(1)−Cl(1)	2.4656(9)	V(3)−C(40)	1.925(4)
V(1)−Cl(2)	2.4701(9)	V(3)−C(41)	1.888(4)
V(1)−Cl(3)	2.4558(9)	V(3)−C(42)	1.920(3)
V(1)−P(1)	2.4804(9)	V(3)−C(43)	1.937(4)
V(1)−P(2)	2.5037(9)	V(3)−P(7)	2.3974(11)
V(1)−P(3)	2.5070(9)	V(3)−P(8)	2.4148(10)
V(2)−Cl(1)	2.4633(9)	C(40)−O(1)	1.166(5)
V(2)−Cl(2)	2.4609(9)	C(41)−O(2)	1.187(5)
V(2)−Cl(3)	2.4529(9)	C(42)−O(3)	1.173(4)
V(2)−P(4)	2.4897(10)	C(43)−O(4)	1.165(5)
V(2)−P(5)	2.5021(9)		
V(2)−P(6)	2.5026(10)		

(42) Ellis, J. E.; Stein, B. K.; Frerichs, S. R. *J. Am. Chem. Soc.* **1993**, *115*, 4066−4075.
(43) Edema, J. J. H.; Stauthamer, W.; van Bolhuis, F.; Gambarotta, S.; Smeets, W. J. J.; Spek, A. L. *Inorg. Chem.* **1990**, *29*, 1302−1306.
(44) Cotton, F. A.; Duraj, S. A.; Manzer, L. E.; Roth, W. J. *J. Am. Chem. Soc.* **1985**, *107*, 3850−3855.
(45) Canich, J. A. M.; Cotton, F. A.; Duraj, S. A.; Roth, W. J. *Polyhedron* **1987**, *6*, 1433−1437.
(46) Cotton, F. A.; Duraj, S. A.; Roth, W. J. *Inorg. Chem.* **1985**, *24*, 913−917.
(47) Calderazzo, F.; De Benedetto, G. E.; Pampaloni, G.; Mössmer, C. M.; Strähle, J.; Wurst, K. *J. Organomet. Chem.* **1993**, *451*, 73−81.
(48) Pampaloni, G.; Englert, U. *Inorg. Chim. Acta* **1995**, *231*, 167−173.
(49) Cotton, F. A.; Duraj, S. A.; Extine, M. W.; Lewis, G. E.; Roth, W. J.; Schmulbach, C. D.; Schwotzer, W. *J. Chem. Soc., Chem. Commun.* **1983**, 1377−1378.
(50) Bouma, R. J.; Teuben, J. H.; Beukema, W. R.; Bansemer, R. L.; Huffman, J. C.; Caulton, K. G. *Inorg. Chem.* **1984**, *23*, 2715−2718.

Table 5. Selected Bond Angles (deg) for [(trimpsi)V(μ-Cl)$_3$V(trimpsi)][(η^2-trimpsi)V(CO)$_4$] in [**8**][**9**]

		[**8**]$^+$	
Cl(1)−V(1)−Cl(2)	86.97(3)	Cl(1)−V(2)−P(4)	93.41(3)
Cl(1)−V(1)−Cl(3)	87.83(3)	Cl(1)−V(2)−P(5)	89.71(3)
Cl(1)−V(1)−P(1)	89.29(3)	Cl(1)−V(2)−P(6)	177.97(4)
Cl(1)−V(1)−P(2)	94.55(3)	Cl(2)−V(2)−Cl(3)	87.34(3)
Cl(1)−V(1)−P(3)	177.03(3)	Cl(2)−V(2)−P(4)	176.66(3)
Cl(2)−V(1)−Cl(3)	87.07(3)	Cl(2)−V(2)−P(5)	94.20(3)
Cl(2)−V(1)−P(1)	94.35(3)	Cl(2)−V(2)−P(6)	91.56(3)
Cl(2)−V(1)−P(2)	177.20(3)	Cl(3)−V(2)−P(4)	89.40(3)
Cl(2)−V(1)−P(3)	90.65(3)	Cl(3)−V(2)−P(5)	177.13(4)
Cl(3)−V(1)−P(1)	176.72(3)	Cl(3)−V(2)−P(6)	93.63(3)
Cl(3)−V(1)−P(2)	90.63(3)	P(4)−V(2)−P(5)	89.09(3)
Cl(3)−V(1)−P(3)	93.82(3)	P(4)−V(2)−P(6)	87.90(3)
P(1)−V(1)−P(2)	88.03(3)	P(5)−V(2)−P(6)	88.76(3)
P(1)−V(1)−P(3)	89.12(3)	V(1)−Cl(1)−V(2)	74.07(3)
P(2)−V(1)−P(3)	87.91(3)	V(1)−Cl(2)−V(2)	74.03(3)
Cl(1)−V(2)−Cl(2)	87.22(3)	V(1)−Cl(3)−V(2)	74.42(3)
Cl(1)−V(2)−Cl(3)	87.94(3)		
		[**9**]$^-$	
C(40)−V(3)−C(41)	87.36(17)	C(42)−V(3)−P(7)	174.69(11)
C(40)−V(3)−C(42)	94.54(15)	C(42)−V(3)−P(8)	88.58(11)
C(40)−V(3)−C(43)	169.71(15)	C(43)−V(3)−P(7)	88.75(1)
C(40)−V(3)−P(7)	83.75(11)	C(43)−V(3)−P(8)	92.71(11)
C(40)−V(3)−P(8)	94.22(12)	P(7)−V(3)−P(8)	89.32(3)
C(41)−V(3)−C(42)	91.98(17)	V(3)−C(40)−O(1)	175.8(3)
C(41)−V(3)−C(43)	85.64(16)	V(3)−C(41)−O(2)	179.1(3)
C(41)−V(3)−P(7)	90.26(14)	V(3)−C(42)−O(3)	177.8(3)
C(41)−V(3)−P(8)	178.31(12)	V(3)−C(43)−O(4)	175.5(3)
C(42)−V(3)−C(43)	96.23(15)		

expected. The neutral 17e complex V(dmpe)$_2$(CO)$_2$[51] exhibits a similar average V−P bond length (2.38 Å) while the V(I) complexes V(dmpe)$_2$(CO)$_2$Me (V−P average = 2.45 Å), V(dmpe)$_2$(CO)$_2$O$_2$CEt (V−P average = 2.49 Å), and [V(dmpe)$_2$(CO)$_2$(MeCN)]$^+$ (V−P average = 2.47 Å) exhibit longer V−P distances.[51,52] The longer V−P bond lengths in **5** (V−P average 2.47 Å) are consistent with the vanadium center in [**9**]$^-$ being more electron rich, and they demonstrate the good π-accepting ability of the NO ligand in **5**. Finally, [**9**]$^-$ exhibits average V−C and C−O distances of 1.92 and 1.17 Å, respectively, almost identical to those exhibited by the parent complex, [V(CO)$_6$]$^-$.[53]

The yield of [**8**][**9**]·3THF was quite small, and full characterization data could not be collected. Its IR spectrum (KBr) reveals ν(CO) absorptions at 1891, 1776, and 1752 cm^{-1}, similar to those reported for [V(CO)$_4$(dmpe)]$^-$.[54] LSIMS spectra for [**8**][**9**]·3THF dissolved in a thioglycerol matrix reveal a strong peak at *m*/*z* 829 with the isotopic distribution expected for [**8**]$^+$, thereby further confirming our formulation. Unfortunately, under no conditions could a parent ion be observed for [**9**]$^-$.

The isolation of [**8**][**9**]·3THF explains why the yield of **7** formed via eq 1 is so low since at least four different vanadium-containing molecules are isolable, and all of them are derived from the reduction of **6**. In the case of [**8**]$^+$ each vanadium center has only been reduced by one electron, in the case of (trimpsi)V(CO)$_3$H the vanadium center has been formally reduced by two electrons, and in the case of **7** and [**9**]$^-$ the vanadium centers have been reduced by four electrons. The isolation of [**9**]$^-$ suggests that **6** is best formulated as (η^2-trimpsi)VCl$_3$(THF). Two other observations support this inference, namely, (1) few seven coordinate vanadium complexes are known[55,56] and (2) the ESR signal of the closely related compound (trimpsi)TiCl$_3$(THF) exhibits coupling to only two phosphorus nuclei.[57]

Table 6. Cyclic Voltammetry Data for (trimpsi)M(CO)$_2$(NO) [M = Nb (**3**), Ta (**4**)]

complex	solvent	$E_{p,a}$, V	scan rate, V/s
3	CH_2Cl_2	−0.71[a]	0.5
	MeCN	−0.96	0.5
4	CH_2Cl_2	−0.55	0.5
	MeCN	−0.54	0.5

[a] All potentials are measured vs [Cp$_2$Fe]$^{0/+}$.

Solution Redox Properties of the (trimpsi)M(CO)$_2$NO Complexes. The solution redox properties of **3**−**5** have been investigated by cyclic voltammetry. Room-temperature cyclic voltammetry data for **3** and **4** are summarized in Table 6. Both **3** and **4** in CH_2Cl_2 exhibit the same cyclic voltammograms regardless of whether positive or negative potentials are scanned first. These traces are relatively complicated and consist of an irreversible oxidation feature followed by several nondistinct oxidation features, and no reduction features, within the solvent window, at all scan rates. Most likely, the first oxidation feature (irreversible even at scan rates of 5 V/s) reflects the formation of [(trimpsi)M(CO)$_2$(NO)]$^+$ (M = Nb, Ta), which are unstable under these conditions. The other nondistinct oxidation features, which appear at higher potentials, presumably involve electron removal from the decomposition products of [(trimpsi)M(CO)$_2$(NO)]$^+$. The cyclic voltammogram traces of **3** and **4** in MeCN are almost identical to those recorded in CH_2Cl_2. Each consists of an irreversible oxidation feature with several nondistinct oxidation features occurring at higher potentials. No change is wrought by increasing the scan rate.

Cyclic voltammograms of **5** in CH_2Cl_2 show a reversible oxidation feature ($E_{1/2}$ = −0.74 V) followed by an irreversible feature (0.61 V at 0.5 V/s) (Table 7). The $i_{p,a}/i_{p,c}$ value for the first oxidation is unity over the whole range of scan rates, establishing its chemical reversibility. Also, plots of $i_{p,a}$ vs $\sqrt{\nu}$ for this feature are linear, indicating that the oxidation is diffusion-controlled. The reversible feature undoubtedly corresponds to the formation of the 17e cation [(trimpsi)V(CO)$_2$(NO)]$^+$ ([**5**]$^+$) (eq 3). The irreversible feature at 0.61 V presumably involves the oxidation of [**5**]$^+$ to a 16e dication, which subsequently decomposes. This second feature is irreversible even at scan rates of 5 V/s. Again, the cyclic voltammograms of **5** in MeCN are identical to those recorded in CH_2Cl_2, the reversible oxidation feature

(51) Wells, F. J.; Wilkinson, G.; Motevalli, M.; Hursthouse, M. B. *Polyhedron* **1987**, *6*, 1351−1360.
(52) Protasiewicz, J. D.; Bianconi, P. A.; Williams, I. D.; Liu, S.; Rao, P.; Lippard, S. J. *Inorg. Chem.* **1992**, *31*, 4134−4142.
(53) Wilson, R. D.; Bau, R. *J. Am. Chem. Soc.* **1974**, *96*, 7601−7602.
(54) Ellis, J. E.; Faltynek, R. A. *J. Organomet. Chem.* **1975**, *93*, 205−217.
(55) Connelly, N. G. In *Comprehensive Organometallic Chemistry*; Abel, E. W., Stone, F. G. A., Wilkinson, G., Eds.; Pergamon Press: New York, 1982; Vol. 3, pp 647−704.
(56) Berno, P.; Gambarotta, S.; Richeson, D. In *Comprehensive Organometallic Chemistry II*; Abel, E. W., Stone, F. G. A., Wilkinson, G., Eds.; Elsevier: New York, 1995; Vol. 5, pp 1−55.
(57) Gardner, T. G. Ph.D. Thesis, University of Illinois at Urbana-Champaign, Urbana, IL, 1989.

Table 7. Electrochemical Parameters for the Oxidation of **5** Relative to $[Cp_2Fe]^{0/+}$

solvent	scan rate, V/s	$E_{p,a}$, V	ΔE_p, V	$E_{1/2}$, V	$i_{p,a}/i_{p,c}$
CH_2Cl_2	0.1	−0.67	0.14	−0.74	1.0
	0.2	−0.66	0.16	−0.74	1.0
	0.5	−0.64	0.20	−0.74	1.0
	0.8	−0.61	0.24	−0.73	1.0
	1.2	−0.60	0.26	−0.73	1.0
	1.5	−0.59	0.28	−0.73	1.0
MeCN	0.1	−0.97	0.08	−1.01	1.1
	0.2	−0.96	0.09	−1.01	1.0
	0.5	−0.95	0.11	−1.01	1.0
	0.8	−0.95	0.11	−1.00	1.0
	1.2	−0.94	0.13	−1.01	1.1
	1.8	−0.94	0.14	−1.01	1.1

having an $E_{1/2}$ value of −1.01 V in this solvent while the irreversible feature occurs at 0.25 V at 0.5 V/s.

$$\underset{\mathbf{5}}{(\text{trimpsi})V(CO)_2(NO)} \rightleftharpoons \underset{[\mathbf{5}]^+}{[(\text{trimpsi})V(CO)_2(NO)]^+} + e^- \quad (3)$$

Few studies concerning the electrochemical properties of niobium and tantalum carbonyl and phosphine complexes have been reported.[58−60] As with **3** and **4**, an irreversible first oxidation is observed for $[Ta(CO)_6]^-$ in CH_2Cl_2.[60] Similarly, the observed electrochemical properties of **5** are comparable to those found for $[V(CO)_6]^-$.[61]

In hindsight, the irreversibility of the first oxidation features for **3** and **4** is not surprising considering the paucity of 17e complexes of the type $M(CO)_x(L)_y$ (M = Nb, Ta; L = neutral Lewis base).[60] In contrast, several 17e organometallic vanadium complexes are known, such as $V(CO)_6$[62] and various phosphine,[51,63,64] arene,[65] and isocyanide derivatives.[66]

[(trimpsi)V(CO)$_2$(NO)][BF$_4$]. The electrochemical reversibility of the $[(\text{trimpsi})V(CO)_2(NO)]^{0/+}$ couple suggested that the bulk synthesis of $[\mathbf{5}]^+$ should be possible. The reaction of **5** with $[Cp_2Fe][BF_4]$ at ambient temperature in CH_2Cl_2 results in an immediate color change from cherry red to orange. An IR spectrum of this solution exhibits two ν(CO) bands at 1977 and 1895 cm^{-1} and one ν(NO) absorption at 1596 cm^{-1}. The increases in both ν(CO) and ν(NO) are consistent with the anticipated decrease in electron density at the metal center, and we attribute these IR spectral features to $[(\text{trimpsi})V(CO)_2(NO)][BF_4]$ ($[\mathbf{5}][BF_4]$). Consistent with the cyclic voltammetry studies, addition of 1 equiv of Cp_2Co to this solution immediately regenerates **5**. X-band ESR spectra of $[\mathbf{5}][BF_4]$ or $[\mathbf{5}\text{-}^{15}N][BF_4]$ generated in situ in CH_2Cl_2 reveal identical 35-line patterns (Figure 9), demonstrating that the nitrogen atom of the NO ligand makes little or no contribution to either spectrum. The hyperfine coupling is due to the ^{51}V ($I = 7/2$) nucleus, the ^{31}P nucleus trans to the nitrosyl, and the two ^{31}P nuclei cis to the nitrosyl. The observed coupling constants are $A(^{51}V) = 56$ G, $A(^{31}P_{trans}) = 15$ G, and $A(^{31}P_{cis}) = 28$ G with $g = 2.0035$. These spectra provide further evidence that $[\mathbf{5}]^+$ is correctly formulated as $[(\text{trimpsi})V(CO)_2(NO)]^+$, as evinced by hyperfine coupling to all three ^{31}P nuclei in the trimpsi ligand. No other signal is evident in the ESR spectra. On standing, though, solutions of $[\mathbf{5}][BF_4]$ begin to darken to red and evolve gas. Similar results are obtained when $[Cp_2Fe][BPh_4]$ is used in place of $[Cp_2Fe][BF_4]$, although it qualitatively appears that $[\mathbf{5}][BPh_4]$ decomposes at a slower rate than the tetrafluoroborate salt. Unfortunately, under no conditions could $[\mathbf{5}][BX_4]$ (X = F, Ph) be isolated. All materials recovered from these reactions were noncrystalline and were devoid of carbonyl or nitrosyl ligands as indicated by their IR spectra.

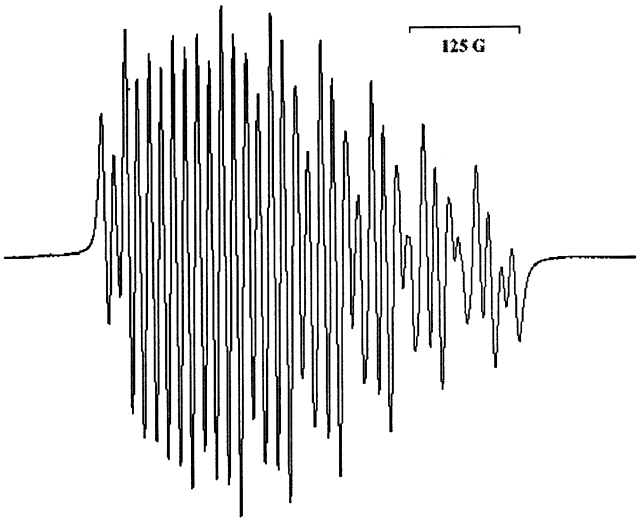

Figure 9. X-band ESR spectrum of $[(\text{trimpsi})V(CO)_2(^{15}NO)][BF_4]$ ($[\mathbf{5}\text{-}^{15}N][BF_4]$) in CH_2Cl_2 at room temperature.

Summary

In this report we have provided full details of the synthesis and characterization of (trimpsi)$M(CO)_2(NO)$ (M = Nb, Ta) and their precursors, (trimpsi)$M(CO)_3I$. In addition, we have also described the preparation of the congeneric vanadium species, (trimpsi)$V(CO)_2(NO)$, and we have outlined the redox properties of all three dicarbonylnitrosyls. In previous work with group 6 nitrosyl complexes we have established that the related $Cp'M(CO)_2(NO)$ complexes (Cp′ = Cp, Cp*; M = Cr, Mo, W) are invaluable precursors to a wide range of inorganic and organometallic derivatives of these elements.[1] We are currently investigating whether the isoelectronic group 5 complexes described in this paper can be utilized similarly to develop the chemistry of group 5 nitrosyls. We shall be reporting the results of these studies of the characteristic chemistry of the (trimpsi)$M(CO)_2(NO)$ (M = V, Nb, Ta) complexes in due course.

Experimental Section

General Methods. All reactions and subsequent manipulations were performed under anaerobic and anhydrous conditions under an atmosphere of dinitrogen or argon. General procedures routinely

(58) Bond, A. M.; Bixler, J. W.; Mocellin, E.; Datta, S.; James, E. J.; Wreford, S. S. *Inorg. Chem.* **1980**, *19*, 1760−1765.
(59) Blaine, C. A.; Ellis, J. E.; Mann, K. R. *Inorg. Chem.* **1995**, *34*, 1552−1561.
(60) Koeslag, M. A.; Baird, M. C.; Lovelace, S.; Geiger, W. E. *Organometallics* **1996**, *15*, 3289−3302.
(61) Bond, A. M.; Colton, R. *Inorg. Chem.* **1976**, *15*, 2036−2040.
(62) Ercoli, R.; Calderazzo, F.; Alberola, A. *J. Am. Chem. Soc.* **1960**, *82*, 2966−2967.
(63) Werner, R. P. M. *Z. Naturforsch., B: Chem. Sci.* **1961**, *16*, 477−478.
(64) Ellis, J. E.; Faltynek, R. A.; Rochfort, G. L.; Stevens, R. E.; Zank, G. A. *Inorg. Chem.* **1980**, *19*, 1082−1085.
(65) Pomije, M. K.; Kurth, C. J.; Ellis, J. E.; Barybin, M. V. *Organometallics* **1997**, *16*, 3582−3587.
(66) Barybin, M. V.; Young, V. G., Jr.; Ellis, J. E. *J. Am. Chem. Soc.* **2000**, *122*, 4678−4691.

employed in these laboratories have been described in detail previously.[67] Tetrahydrofuran was distilled from molten potassium, while dichloromethane, 1,2-dimethoxyethane (DME), and acetonitrile were distilled from calcium hydride. CD_2Cl_2 was dried by standing over activated 4 Å molecular sieves for 2 days and degassed prior to use. CD_3CN was distilled from calcium hydride. $[NO][BF_4]$ was purchased from Aldrich and was sublimed under dynamic vacuum before use. $[Et_4N][V(CO)_6]$,[68] $[Et_4N][M(CO)_6]$ (M = Nb, Ta),[69] the tripodal phosphine, ^{t}BuSi(CH$_2$PMe$_2$)$_3$,[70] $[^{15}NO][BF_4]$,[71] and $[Cp_2Fe][BPh_4]$[72] were prepared by published procedures. All other reagents were purchased from commercial suppliers and were used as received.

NMR spectra were recorded on Bruker AMX 500, AVA 300, or AVA 400 spectrometers. ^{1}H and ^{13}C spectra are referenced to external $SiMe_4$ using the residual protio solvent peaks as internal standards (^{1}H NMR experiments) or the characteristic resonances of the solvent nuclei (^{13}C NMR experiments). ^{31}P spectra are referenced to external 85% H_3PO_4. ^{51}V spectra are referenced to external VCl_3O (neat), while ^{93}Nb spectra are referenced to external $KNbCl_6$ in CD_3CN (saturated solution). Where appropriate, NMR spectral assignments were confirmed by conventional homonuclear and heteronuclear correlation spectroscopy experiments. All ESR spectra were recorded on a Varian E-3 spectrometer. Data were analyzed using Bruker Winepr software. All assignments were verified by simulating the spectra using Bruker Simfonia software.

Cyclic Voltammetry Measurements. The customary methodology employed during cyclic voltammetry (CV) studies in these laboratories has been outlined in detail elsewhere.[73] CV experiments were performed using a Pine Instrument Company AFCBP1 Bipotentiostat, and the data were processed using PINECHEM 2.7 software. The working electrode consisted of a platinum bead embedded in glass (~1 mm diameter), the counter electrode was a platinum wire, and the reference electrode consisted of AgCl plated on Ag wire. The solutions employed during CV studies were typically 3 mM in the organometallic complex and 0.1 M in $[Bu_4N][PF_6]$, and they were maintained under an atmosphere of Ar. All potentials are reported versus the $[Cp_2Fe]^{0/+}$ couple. For all trials $i_{p,a}/i_{p,c} = 1$ for the $[Cp_2Fe]^{0/+}$ couple, while $i_{p,c}$ increased linearly with the square root of the scan rate (i.e. $\sqrt{\nu}$). Redox couples which exhibited behavior similar to the $[Cp_2Fe]^{0/+}$ couple were thus considered reversible.

Preparation of (trimpsi)Nb(CO)$_3$I (1). To a rapidly stirred solution of $[Et_4N][Nb(CO)_6]$ (6.6 g, 16.9 mmol) in DME (500 mL) at −78 °C was added a solution of I_2 (4.3 g, 16.9 mmol) in THF (50 mL) via a fine bore cannula. The evolution of CO gas accompanied the addition, and the initially orange solution darkened to a turbid red color. The stirred mixture was allowed to warm to −50 °C over a period of 30 min. Trimpsi (6.3 mL, 16.9 mmol) was then added to the cold mixture, whereupon the solution immediately lightened to a turbid yellow-orange color. The mixture was permitted to warm slowly to room temperature before being heated to reflux for 2 h. Stirring was ceased to allow a white precipitate to settle, and the mixture was then rapidly filtered while hot through a plug of Celite (3 × 3 cm) to obtain a clear blood-red filtrate. Upon cooling this filtrate slowly to room temperature, analytically pure **1** was deposited as a mass of red microcrystals. A second crop of **1** was obtained by reducing the volume of the mother liquor and cooling the remaining solution to −30 °C overnight. Yield: 8.5 g, 82%.

Anal. Cald for $C_{16}H_{33}INbO_3P_3Si$: C, 31.27; H, 5.37. Found: C, 31.28; H, 5.50. IR (Nujol mull): ν(CO) 1938 (s), 1846 (s), 1800 (s) cm^{-1}. ^{1}H NMR (500 MHz, CD_2Cl_2, 25 °C): δ 0.90 (d, $^2J_{PH}$ = 10.5 Hz, 3 CH$_2$), 0.91 (s, CMe$_3$), 1.58 (d, $^2J_{PH}$ = 6.3 Hz, 3 PMe$_2$). ^{13}C{^{1}H} (125 MHz, CD_2Cl_2, 25 °C): δ 9.5 (s, 3 CH$_2$), 17.2 (s, CMe$_3$), 22.8 (d, $^1J_{PC}$ = 20 Hz, 3 PMe$_2$), 25.7 (s, C*Me*$_3$), CO resonances not observed. ^{31}P{^{1}H} (202 MHz, CD_2Cl_2, 25 °C): δ −17.8 (br s, $W_{1/2}$ = 1100 Hz, 3 PMe$_2$).

Preparation of (trimpsi)Ta(CO)$_3$I (2). Complex **2** was prepared by following a procedure entirely analogous to that outlined in the preceding section. Yield: 84%.

Anal. Calcd for $C_{16}H_{33}IO_3P_3SiTa$: C, 27.35; H, 4.70. Found: C, 27.74; H, 4.82. IR (Nujol mull): ν(CO) 1928 (s), 1838 (s), 1793 (s) cm^{-1}. ^{1}H NMR (500 MHz, CD_2Cl_2, 25 °C): δ 0.90 (s, CMe$_3$), 0.95 (d, $^2J_{PH}$ = 11.0 Hz, 3 CH$_2$), 1.69 (d, $^2J_{PH}$ = 6.8 Hz, 3 PMe$_2$). ^{13}C{^{1}H} (125 MHz, CD_2Cl_2, 25 °C): δ 9.0 (s, 3 CH$_2$), 17.3 (s, *C*Me$_3$), 23.4 (d, $^1J_{PH}$ = 24 Hz, 3 PMe$_2$), 25.8 (s, C*Me*$_3$), CO resonances not observed. ^{31}P{^{1}H} (202 MHz, CD_2Cl_2, 25 °C): δ −32.98 (br s, $W_{1/2}$ = 550 Hz, 3 PMe$_2$).

Preparation of (trimpsi)Nb(CO)$_2$(NO) (3). A slurry of **1** (4.0 g, 6.5 mmol) in DME (250 mL) was transferred into a flask that contained a Hg amalgam of Na (0.34 g, 15 mmol, excess), and the contents were then stirred at room temperature overnight. The initially red mixture became a clear orange-yellow solution in which a finely divided white precipitate was suspended. The solution was cannulated into a clean vessel and was cooled to −78 °C. A solution of Diazald (1.4 g, 6.5 mmol) in THF (30 mL) was added slowly with stirring, whereupon gas was evolved and the reaction mixture darkened to a deep purple color. As the mixture warmed slowly to room temperature, a gelatinous white precipitate appeared. Stirring was ceased, and the contents were allowed to settle for a period of 4 h at room temperature. The final mixture was then filtered through a plug of Celite (3 × 4 cm), and the Celite was washed with DME (2 × 20 mL). The volume of the filtrate was reduced in vacuo to 100 mL. Slow cooling of this solution to −30 °C overnight induced the deposition of a mass of burgundy crystals which desolvated upon exposure to vacuum. Recrystallization of this solid from THF/hexanes (2:1) afforded analytically pure **3**. Yield: 2.8 g, 88%.

Anal. Calcd for $C_{15}H_{33}NNbO_3PSi$: C, 36.81; H, 6.75; N, 2.86. Found: C, 36.94; H, 6.65; N, 2.97. IR (Nujol mull): ν(CO) 1908 (s), 1821 (s) cm^{-1}; ν(NO) 1518 (s) cm^{-1}. ^{1}H NMR (500 MHz, CD_2Cl_2, 25 °C): δ 0.66 (d, $^2J_{PH}$ = 9.9 Hz, CH$_2$), 0.80−1.00 (overlapping m, 2 CH$_2$), 0.89 (s, CMe$_3$), 1.25 (d, $^2J_{PH}$ = 4.4 Hz, PMe$_2$), 1.56 (br s, 2 PMe$_2$). ^{13} C{^{1}H} (125 MHz, CD_2Cl_2, 25 °C): δ 9.7 (s, CH$_2$), 10.8 (s, 2 CH$_2$), 17.38 (q, $^3J_{PC}$ = 6 Hz, *C*Me$_3$), 19.7 (br s, 2 PMe), 20.3 (d, $^1J_{PC}$ = 14 Hz, PMe$_2$), 23.9 (vt, J = 11 Hz, 2 PMe), 25.9 (s, C*Me*$_3$), CO resonances not observed. ^{31}P{^{1}H} (202 MHz, CD_2Cl_2, 25 °C): δ −20 ($W_{1/2}$ = 5600 Hz). ^{93}Nb{^{1}H} (98 MHz, CD_2Cl_2, 25 °C): δ −1493 ($W_{1/2}$ = 4800 Hz).

Preparation of (trimpsi)Ta(CO)$_2$(NO) (4). Complex **4** was prepared by following a procedure entirely analogous to that described above for **3**. Yield: 90%.

Anal. Calcd for $C_{15}H_{33}NO_3PSiTa$: C, 31.20: H, 5.72; N, 2.43. Found: C, 31.30; H, 5.79; N, 2.32. IR (Nujol mull): ν(CO) 1895 (s), 1802 (s) cm^{-1}; ν(NO) 1515 (s) cm^{-1}. ^{1}H NMR (500 MHz,

(67) Legzdins, P.; Rettig, S. J.; Ross, K. J.; Batchelor, R. J.; Einstein, F. W. B. *Organometallics* **1995**, *14*, 5579−5587.
(68) Barybin, M. V.; Pomije, M. K.; Ellis, J. E. *Inorg. Chim. Acta* **1998**, *269*, 58−62.
(69) Ellis, J. E.; Warnock, G. F. P.; Barybin, M. V.; Pomije, M. K. *Chem.−Eur. J.* **1995**, *1*, 521−527.
(70) Girolami, G. S. Personal communication.
(71) Connelly, N. G.; Dragget, P. T.; Green, M.; Kuc, T. A. *J. Chem. Soc., Dalton Trans.* **1977**, 70−73.
(72) Aggarwal, R. P.; Connelly, N. G.; Crespo, M. C.; Dunne, B. J.; Hopkins, P. M.; Orpen, A. G. *J. Chem. Soc., Dalton Trans.* **1992**, 655−662.
(73) Herring, F. G.; Legzdins, P.; Richter-Addo, G. B. *Organometallics* **1989**, *8*, 1485−1493.

CD_2Cl_2, 25 °C): δ 0.74 (d, $^2J_{PH}$ = 10.6 Hz, CH_2), 0.80−1.10 (overlapping m, 2 CH_2), 0.89 (s, CMe_3), 1.36 (d, $^2J_{PH}$ = 4.6 Hz, PMe_2), 1.63 (br s, 2 PMe), 1.68 (br s, 2 PMe). $^{13}C\{^1H\}$ (125 MHz, CD_2Cl_2, 25 °C): δ 9.4 (s, CH_2), 10.4 (s, 2 CH_2), 17.3 (q, $^3J_{PC}$ = 6 Hz, CMe_3), 19.8 (br s, 2 PMe), 21.0 (d, $^1J_{PC}$ = 17 Hz, PMe_2), 24.7 (vt, J = 14 Hz, 2 PMe), 26.0 (s, CMe_3), 247.2 (2 CO). $^{31}P\{^1H\}$ (202 MHz, CD_2Cl_2, 25 °C): δ −33.2 (1 PMe_2), −24.0 (2 PMe_2).

Preparation of (trimpsi)V(CO)$_2$(NO) (5). To a rapidly stirred suspension of finely ground [NO][BF_4] (0.65 g, 5.6 mmol) in CH_2Cl_2 (100 mL) at −35 °C was added finely ground [Et_4N][$V(CO)_6$] (1.91 g, 5.5 mmol) via a powder funnel. The addition caused a color change from yellow to purple over the course of 30 min and the concomitant evolution of CO gas. The reaction mixture was kept at −35 °C for 8 h after which trimpsi (1.8 mL, 4.8 mmol) was added via syringe, and the rapidly stirred purple solution was allowed to warm to room temperature, whereupon it became bright orange. The CH_2Cl_2 was removed in vacuo, THF (30 mL) was added via syringe, and the orange solution was refluxed for 1 h. The final cherry-red solution was filtered through a plug of Celite (3 × 1 cm) supported on a medium-porosity frit, and the plug was subsequently washed with THF (2 × 10 mL). The THF was removed from the combined filtrates in vacuo to obtain a brown oil. Addition of MeCN (40 mL) by cannula onto the oil gave a red-brown solution. The volume of this solution was reduced in vacuo to 20 mL, and the concentrated solution was cooled to −30 °C overnight to induce the deposition of **5** as cherry red crystals (1.45 g, 59%). (trimpsi)$V(CO)_2(^{15}NO)$ (**5-**^{15}N) was prepared in comparable yields using [^{15}NO][BF_4].

Anal. Calcd for $C_{15}H_{33}NO_3P_3SiV$: C, 40.27; H, 7.43; N, 3.13. Found: C, 40.17; H, 7.49; N, 3.01. IR (Nujol mull) ν(CO): 1910 (s), 1920 (s) cm^{-1}, ν(NO) 1543 (s) cm^{-1}. ^1H NMR (500 MHz, CD_2Cl_2, 25 °C): δ 0.61 (d, J_{PH} = 10.4 Hz, CH_2), 0.75 (m, CH_2), 0.85 (m, CH_2), 0.88 (s, CMe_3), 1.28 (d, J_{PH} = 5.0 Hz, PMe_2), 1.51 (br s, 2 PMe), 1.53 (br s, 2 PMe). $^1H\{^{31}P\}$ (500 MHz, CD_2Cl_2, 25 °C): δ 0.61 (s, CH_2), 0.75 (d, J_{HH} = 20.1 Hz, CH_2), 0.85 (d, J_{HH} = 20.1 Hz, CH_2), 0.88 (s, CMe_3), 1.28 (s, PMe_2), 1.51 (s, 2 PMe), 1.53 (s, 2 PMe). $^{13}C\{^1H\}$ (125 MHz, CD_2Cl_2, 25 °C): δ 8.8 (s, CH_2), 9.7 (s, CH_2), 17.2 (q, J_{CP} = 6.3 Hz, CMe_3), 19.5 (br s, 2 PMe), 20.9 (d, J_{CP} = 12.5 Hz, PMe_2), 23.7 (vt, J_{CP} = 12.5 Hz, 2 PMe), 26.0 (s, CMe_3). $^{31}P\{^1H\}$ (202 MHz, CD_2Cl_2, 25 °C): δ −10.0 (octet, J_{PV} = 130 Hz, 1P), 5.0 (octet, J_{PV} = 220 Hz, 2P). MS (EI, 150 °C): m/z 447, [P^+].

Preparation of (trimpsi)VCl_3(THF) (6). Girolami and coworkers first reported this compound, but no synthetic details were provided.[18] To a rapidly stirred suspension of $VCl_3(THF)_3$ (6.6 g, 17.6 mmol) in THF (200 mL) at room temperature was added trimpsi (6.6 mL, 17.7 mmol). The color quickly changed from red to blue, and after 15 min a green precipitate began to form. The reaction mixture was stirred for 16 h, and the precipitate was then allowed to settle. The supernatant solution was cannulated away from the solid and discarded. The remaining green powder was washed with pentane (50 mL) and dried in vacuo for 2 h. Yield: 7.6 g, 80%. Anal. Calcd for $C_{17}H_{41}Cl_3OP_3SiV$: C, 37.83; H, 7.66. Found: C, 37.49; H, 7.61.

Preparation of [Et_4N][(trimpsi)$V(CO)_3$] (7). To a solution of sodium naphthalenide, prepared from Na (0.49 g, 21.3 mmol) and naphthalene (2.8 g, 21.8 mmol) in THF (300 mL) at −78 °C in a thick-walled glass bomb, was added a suspension of **6** (2.5 g, 4.6 mmol) in THF (200 mL). The original green solution quickly became red-brown. CO (1.5 atm) was introduced into the bomb, the solution was allowed to warm to room temperature in the absence of light, and the mixture was stirred for 24 h at ambient temperature. The final mixture was filtered through a plug of Celite (3 × 3 cm) into a flask containing [Et_4N][Cl] (0.58 g, 3.50 mmol), and the Celite was rinsed with THF (50 mL). The resulting solution was stirred for a further 24 h, at which point the THF was removed in vacuo and the resulting yellow-brown powder was rinsed with hexanes (2 × 60 mL). The solid was redissolved in THF (100 mL), and the solution was refiltered through a plug of Celite (2 × 2 cm). The volume of the filtrate was reduced in vacuo to induce the precipitation of yellow microcrystals of **7**. Yield: 0.14 g (5%). The supernatant solution was again concentrated in vacuo to induce the precipitation of a yellow-green powder which proved to be slightly impure (trimpsi)$V(CO)_3H$ as judged by ^1H NMR spectroscopy (yield: 0.73 g, 35%). Attempted recrystallization of the impure (trimpsi)$V(CO)_3H$ from THF at −30 °C afforded [(trimpsi)V(μ-Cl)$_3$V(trimpsi)][(η^2-trimpsi)$V(CO)_4$]·3THF ([**8**][**9**]·3THF) as green crystals (yield: 8 mg, 0.4%). Reduction of the volume of this solution in vacuo and subsequent cooling afforded yellow needles of (trimpsi)$V(CO)_3H$.

Complex 7 Data. Anal. Calcd for $C_{24}H_{53}NO_3P_3SiV$: C, 50.08; H, 9.28; N, 2.43. Found: C, 50.08; H, 9.35; N, 2.58. IR (Nujol mull): ν(CO) 1780(s), 1680 (s), 1655 (s) cm^{-1}. ^1H NMR (500 MHz, CD_3CN, 25 °C): δ 0.64 (br s, 3 CH_2), 0.78 (s, CMe_3), 1.20 (t of t, J_{NH} = 1.8 Hz, $N(CH_2CH_3)_4$), 1.36 (br s, 6 PMe), 3.18 (q, $N(CH_2CH_3)_4$). $^{13}C\{^1H\}$ (125 MHz, CD_3CN, 25 °C): δ 7.8 (s, $N(CH_2CH_3)_4$), 13.5 (br s, 3 CH_2), 17.5 (s, CMe_3), 26.6 (s, CMe_3), 27.2 (br s, 6 PMe), 53.1 (t, J_{NC} = 3.8 Hz, $N(CH_2CH_3)_4$). $^{31}P\{^1H\}$ (202 MHz, CD_3CN, 25 °C): δ 14.20 (octet, J_{PV} = 200 Hz). MS (EI, 120 °C): m/z 445, [P^+].

Complex [8][9]·3THF Data. IR (KBr): ν(CO) 1891(s), 1776-(s), 1752 (s) cm^{-1}. MS (LSIMS, thioglycerol matrix): m/z 829, [P^+] [for [**8**]$^+$].

X-ray Diffraction Studies. Data collection for each structure was carried out on a Rigaku/ADSC CCD diffractometer using graphite-monochromated Mo Kα radiation. Data collection for **3** and **4** was carried out at −93(1) °C, while data collection for **2**·$^1/_2$THF, **5**, and [**8**][**9**]·3THF was done at −100(1) °C.

Data for **2**·$^1/_2$THF were collected to a maximum 2θ value of 59.2° in 0.50° oscillations with 19.0 s exposures. The solid-state structure of **2**·$^1/_2$THF was solved by direct methods[74] and expanded using Fourier techniques.[75] The material crystallizes with one disordered molecule of THF and what appears to be a disordered hexane, though it could not be positively identified. The disorder in the latter solvent molecule could not be modeled, and as a result, the SQUEEZE function from the PLATON program[76] was used to correct the data for residual electron density found in void spaces in the crystal lattice. Hydrogen atoms were included but not refined. The final cycle of full-matrix least-squares refinement was based on 7073 observed reflections and 255 variable parameters.

For **3**, the data were collected to a maximum 2θ value of 60.1° in 0.50° oscillations with a 35.0 s exposure. The solid-state structure of **3** was solved by direct methods[77] and expanded using Fourier techniques.[75] The molecule is 1:1 disordered with respect to the crystallographic mirror plane. The disordered $-CH_2PMe_2$ moieties could not be fully resolved, and the carbon atoms were refined as

(74) *SIR97*: Altomare, A.; Burla, M. C.; Cammalli, G.; Cascarano, M.; Giacovazzo, C.; Guagliardi, A.; Moliterni, A. G. G.; Polidori, G.; Spagna, A. *J. Appl. Crystallogr.* **1999**, *32*, 115−119.
(75) *DIRDIF94*: Beurskens, P. T.; Admiraal, G.; Beurskens, G.; Bosman, W. P.; de Gelder, R.; Israel, R.; Smits, J. M. M. *The DIRDIF-94 program system*; Technical Report of the Crystallography Laboratory; University of Nijmegen: Nijmegen, The Netherlands, 1994.
(76) *PLATON*: Spek, A. L. *A Multipurpose Crystallographic Tool*; Utrecht University: Utrecht, The Netherlands, 2001.
(77) *SIR92*: Altomare, A.; Cascarano, M.; Giacovazzo, C.; Guagliardi, A. *J. Appl. Crystallogr.* **1993**, *26*, 343.

Table 8. X-ray Crystallographic Data for Complexes **2**·$^1/_2$THF, **3**−**5**, and [**8**][**9**]·3THF

	2·1/2THF	**3**	**4**	**5**	[**8**][**9**]·3THF
			Crystal Data		
empirical formula	$C_{18}H_{37}IO_{3.5}P_3SiTa$	$C_{15}H_{33}NNbO_3P_3Si$	$C_{15}H_{33}NO_3P_3SiTa$	$C_{15}H_{33}NO_3P_3SiV$	$C_{55}H_{123}Cl_3O_7P_9Si_3V_3$
cryst habit, color	platelet, red	prism, dark	irregular, red	platelet, orange-red	platelet, green
cryst size (mm)	0.35 × 0.35 × 0.08	0.25 × 0.35 × 0.40	0.20 × 0.35 × 0.45	0.20 × 0.20 × 0.04	0.30 × 0.15 × 0.07
cryst system	monoclinic	orthorhombic	monoclinic	orthorhombic	triclinic
space group	*C*2/*c*	*Pnma*	$P2_1/n$	$Pna2_1$	$P\bar{1}$
volume (Å^3)	6159.3(2)	2348.8(4)	2386.0(4)	2273.9(4)	3971.8(2)
a (Å)[a]	37.2045(6)	16.5158(10)	9.7532(14)	16.453(2)	10.6262(2)
b (Å)	9.7244(3)	13.6408(8)	17.5506(15)	10.246(1)	18.9290(4)
c (Å)	17.9893(4)	10.426(2)	14.2268(5)	13.488(1)	20.7077(6)
α (deg)	90	90	90	90	83.072(6)
β (deg)	108.8490(8)	90	101.539(1)	90	82.975(6)
γ (deg)	90	90	90	90	74.774(5)
Z	8	4	4	4	2
fw (g/mol)	738.35	489.34	577.39	447.38	1518.78
D (calcd) (Mg/m^3)	1.592	1.384	1.607	1.307	1.270
abs coeff (cm^{-1})	47.77	7.80	48.70	7.12	7.14
F_{000}	2864	1016	1144	944	1612
radiatn, *λ* (Å)	Mo Kα, 0.710 69 Å	Mo Kα, 0.710 69 Å	Mo Kα, 0.710 69 Å	Mo Kα, 0.710 69 Å	MoKα, 0.71069 Å
			Data Refinement		
final R indices[b]	$R_1 = 0.025$, $wR_2 = 0.077$	$R_1 = 0.053$, $wR_2 = 0.140$	$R_1 = 0.049$, $wR_2 = 0.116$	$R_1 = 0.045$, $wR_2 = 0.144$	$R_1 = 0.045$, $wR_2 = 0.128$
goodness-of-fit on F^2[c]	0.88	0.997	0.964	0.96	0.97
largest diff peak and hole[d] (e Å^{-3})	1.61 and 1.67	0.95 and 1.57	3.79 and 3.09	0.97 and 0.99	0.68 and 0.55

[a] Cell dimensions based on the following: **2**·$^1/_2$THF, 17 433 reflections, 5.9° ≤ 2*θ* ≤ 59.2°; **3**, 16 152 reflections, 4.0° ≤ 2*θ* ≤ 60.1°; **4**, 17 441 reflections, 5.0° < 2*θ* < 61.3°; **5**, 17 357 reflections, 6.4° ≤ 2*θ* ≤ 50.1°; [**8**][**9**]·3THF, 15 773 reflections, 4.5° ≤ 2*θ* ≤ 55.8°. [b] Number of observed reflections: **2**·$^1/_2$THF, 2480 [$I_o > 2\sigma(I_o)$]; **3**, 2322, [$I_o > 2\sigma(I_o)$]; **4**, 4227 [$I_o > 2\sigma(I_o)$]; **5**, 2485 [$I_o > 3\sigma(I_o)$]; [**8**][**9**]·3THF, 11 150 [$I_o > 2\sigma(I_o)$]. $R_F = \Sigma(|F_o| - |F_c|)/\Sigma|F_o|$. wR_F: **2**·$^1/_2$THF, **5**, and [**8**][**9**]·3THF, $[\Sigma((|F_o|^2 - |F_c|^2)^2)/\Sigma wF_o^4]^{1/2}$; **3** and **4,** $[\Sigma(w(|F_o|^2 - |F_c|^2)^2)/\Sigma wF_o^4]^{1/2}$. *w*: **2**·$^1/_2$THF and **3**, $[\sigma^2F_o^2]^{-1}$; **4**, $[\sigma_c^2(F_o^2) + p^2/4(F_o^2)]^{-1}$, $p = 0.0200$; **5**, $[\sigma^2F_o]^{-1}$; [**8**][**9**]·3THF, $[\sigma_c^2(F_o^2) + (0.0629P)^2]^{-1}$, $P = (\max(F_o^2, 0) + 2F_c^2)/3$. [c] GOF = $[\Sigma(w(|F_o| - |F_c|)^2)/\text{degrees of freedom}]^{1/2}$. [d] **3** near Nb; **4** near Ta.

split atoms. As a result of the disorder, the geometry shows some deviation from expected values. The 0.5 occupancy Me carbon atom C(5a) was refined isotropically because the anisotropic thermal parameters were nonpositive definite. All other non-hydrogen atoms were refined anisotropically. Restraints were employed to ensure that all disordered Si−C and P−C bonds have similar distances. The structure was refined with one CO ligand lying on the mirror plane while the remaining two nonphosphine ligand sites were refined as being occupied each by 0.5 NO and 0.5 CO ligands. The final cycle of full-matrix least-squares refinement was based on all 3483 unique reflections and 155 variable parameters.

Data for **4** were collected to a maximum 2*θ* value of 61.3° in 0.50° oscillations with 70.0 s exposures. The solid-state structure of **4** was solved by heavy-atom Patterson methods[78] and expanded using Fourier techniques.[75] The non-hydrogen atoms were refined anisotropically, and hydrogen atoms were fixed in calculated positions with C−H = 0.98 Å. During the refinement fragments of NO and CO ligands were found at each of the three nonphosphine ligand sites. The populations of the NO fragments were determined by refining each of them such that the sum of their populations equaled 1. The three CO fragments were refined such that NO + CO at each position equaled 1. All N−O distances were restrained to the same value, as were the C−O distances. The final cycle of full-matrix least-squares refinement was based on all 6039 reflections and 217 variable parameters.

Data for **5** were collected to a maximum 2*θ* value of 50.1° in 0.50° oscillations with 35.0 s exposures. The solid-state structure of **5** was solved by direct methods[74] and expanded using Fourier techniques.[75] The non-hydrogen atoms were refined anisotropically. Hydrogen atoms were included but not refined. Distinguishing the lone nitrosyl ligand from the two carbonyl ligands was done as follows. All three ligands were originally labeled as carbonyls. Two ligands had V−C distances of 1.8 Å, roughly halfway between the expected V−C and V−N distances (1.9 and 1.7 Å, respectively). The remaining ligand was 1.9 Å from the V. As a result, the possibility of one CO and one NO partially occupying two sites was investigated. In the end there was no evidence to suggest any disorder. Next, all three ligands were again labeled as CO, and the populations of all three C's were refined. The population of one carbon refined to approximately 1.2, while the populations of the remaining two carbons remained almost exactly 1. The final cycle of full-matrix least-squares refinement was based on 3861 observed reflections and 216 variable parameters.

For [**8**][**9**]·3THF, the data were collected to a maximum 2*θ* value of 55.8° in 0.50° oscillations with 55.0 s exposures. The solid-state structure of [**8**][**9**]·3THF was solved by direct methods[74] and expanded using Fourier techniques.[75] The material crystallizes with three molecules of THF in the asymmetric unit. One of these THF's was disordered and refined in two orientations, using restraints on bond distances to maintain a reasonable geometry. The atoms of this disordered THF were refined isotropically. A second THF was severely disordered and could not be properly modeled. As a result, the SQUEEZE function from the PLATON program[76] was used to correct the observed data for residual electron density in the space occupied by the disordered THF. Hydrogen atoms were included but not refined. The final cycle of full-matrix least-squares refinement was based on 16 180 observed reflections and 699 variable parameters.

For all five structure solutions and refinements, neutral atom scattering factors were taken from Cromer and Waber.[79] Anomalous

(78) *PATTY*: Beurskens, P. T.; Admiraal, G.; Beurskens, G.; Bosman, W. P.; Garcia-Granda, S.; Gould, R. O.; Smits, J. M. M.; Smykalla, C. *The DIRDIF program system*; Technical Report of the Crystallography Laboratory; University of Nijmegen: Nijmegen, The Netherlands, 1992.

(79) Cromer, D. T.; Waber, J. T. *International Tables for X-ray Crystallography*; Kynoch Press: Birmingham, U.K., 1974; Vol. IV.

dispersion effects were included in F_{calc};[80] the values for $\Delta f'$ and $\Delta f''$ were those of Creagh and McAuley.[81] The values for the mass attenuation coefficients are those of Creagh and Hubbell.[82] All data sets were corrected for Lorentz and polarization effects. All calculations were performed using the *teXsan*[83] crystallographic software package of Molecular Structure Corp. and/or SHELXL97.[84] X-ray crystallographic data for all five complexes are collected in Table 8, and full details of all crystallographic analyses are provided as Supporting Information.

(80) Ibers, J. A.; Hamilton, W. C. *Acta Crystallogr.* **1964**, *17*, 781−782.
(81) Creagh, D. C.; McAuley, W. J. *International Tables of X-ray Crystallography*; Wilson, A. J. C., Ed.; Kluwer Academic Publishers: Boston, MA, 1992; Vol. C, pp 219−222.
(82) Creagh, D. C.; Hubbell, J. H. *International Tables for X-ray Crystallography*; Wilson, A. J. C., Ed.; Kluwer Academic Publishers: Boston, MA, 1992; Vol. C, pp 200−206.
(83) *teXsan*: *Crystal Structure Analysis Package*; Molecular Structure Corp.: The Woodlands, TX, 1985 and 1992.
(84) Sheldrick, G. M. *SHELXL97*; University of Göttingen: Göttingen, Germany, 1997.

Acknowledgment. We are grateful to the Natural Sciences and Engineering Research Council of Canada for support of this work in the form of grants to P.L. and postgraduate scholarships to T.W.H. We also thank Mr. B. Liboiron for assistance with the acquisition of the ESR data and a reviewer for insightful comments concerning the mutual disorder of the NO and CO ligands in complexes **3** and **4**. P.L. gratefully acknowledges The Canada Council for the Arts for the award to him of a Killam Research Fellowship.

Supporting Information Available: Listings of crystallographic information, atomic coordinates and B_{eq} values, anisotropic thermal parameters, and intramolecular bond distances, angles, and torsion angles in CIF format. This material is available free of charge via the Internet at http://pubs.acs.org.

IC020041R